



Metaheuristic inspired on owls behavior applied to heat exchangers design

Emerson Hochsteiner de Vasconcelos Segundo^{a,*}, Viviana Cocco Mariani^{a,b}, Leandro dos Santos Coelho^{b,c}



^a Department of Mechanical Engineering, Pontifical Catholic University of Paraná (PUCPR), Curitiba, PR, Brazil

^b Department of Electrical Engineering, Federal University of Paraná (UFPR), Curitiba, PR, Brazil

^c Industrial and Systems Engineering Graduate Program (PPGEPS), Pontifical Catholic University of Paraná (PUCPR), Curitiba, PR, Brazil

ARTICLE INFO

Keywords:

Owl Optimization Algorithm
Metaheuristics
Swarm intelligence
Heat exchangers
Multi-objective optimization

ABSTRACT

The main goal of this paper is to propose a novel simple metaheuristic optimizer relate to the swarm intelligence field based on the decoy behavior of owls that has just five main steps and simple control parameters to tune, called Owl Optimization Algorithm (OOA). The main inspiration of OOA is the decoy behavior of the owls when any kind of danger is detected near the nests. The main reasons of using OOA are its high efficiency with fast convergence speed to single-objective optimization problems. The effectiveness of the proposed OOA is demonstrated on a set of well-known mathematical benchmark functions for single-objective and multi-objective optimization and engineering case studies focusing on heat exchangers. The results to mathematical benchmark functions show that OOA converges quickly to the optimal solution with competitive runtime compared with other algorithms of literature for single-objective functions. For multi-objective functions the results showed that the proposed algorithm reaches competitive performance metrics regarding capacity, convergence, diversity and convergence-diversity. When applied in heat exchangers cases, the OOA achieved better results for the objective functions adopted, total cost for both shell-and-tube heat exchanger case studies for single-objective optimization (with 28.17% and 57.78% of reduction in total cost respectively for each case) and good results in comparison with previous works when applied to multi-objective optimization of heat exchangers.

1. Introduction

In engineering and science applications most of the optimization problems are governed by a large number of decision variables, consisting in large scale global optimization problems [1]. The solution of optimization problems can either be from stochastic or deterministic methods. Stochastic methods present a probabilistic warranty of achieving the global solution since their convergence theory usually states that the global minimum will be reached at some point considering infinite time with probability one. On the other hand, deterministic methods ensure that after a finite time an approximation of a global minimizer will be found accordingly to some prescribed tolerances [2]. Metaheuristics constitute an important part in the global optimization algorithms and are often nature-inspired and population-based, using many interacting candidate solutions (individuals) to perform the optimization [3].

One the most popular stochastic technique is the Genetic Algorithm (GA) [4] which proposal aimed the solution of the aforementioned problems for the deterministic techniques. The success of GA consisted

in the selection, reproduction and mutation that are ruled by stochastic behaviors assisting the algorithm to avoid local minima. Since the probability of selection and reproduction of the better individuals are much higher than the worst ones the overall average fitness of the population is improved over the generations. Nowadays, the GA have been applied in a wide range of fields [5].

Among the metaheuristics methods of optimization, those categorized as swarm intelligence where Particle Swarm Optimization (PSO) emerge as the major example [6] appears to be prolific. Swarm intelligence is the property of a system to uses the interaction of the individuals, respecting some kind of behavior causing coherent functional emerging global patterns [7]. The inspiration of swarm intelligence can be found in many nature phenomena, such as colonies foraging, bird flocking, animal herding, bacterial growth, honey bees, fishing schooling and many other. Please see the reference [8] for more details about those techniques.

Aspects mentioned previously fostered many researchers around the world to apply such techniques in engineering problems, where a special attention must be given to heat exchangers. Heat exchangers are

* Corresponding author.

E-mail addresses: e.hochsteiner@gmail.com (E.H.d. Vasconcelos Segundo), viviana.mariani@pucpr.br (V.C. Mariani), leandro.coelho@pucpr.br (L.d.S. Coelho).

Nomenclature	
a_1	numerical constant (€)
a_2	numerical constant (€/m ²)
a_3	numerical constant
A	heat exchanger surface area (m ²)
ABC	Artificial Bee Colony
A_{tot}	heat exchanger surface area (m ²)
B	baffles spacing (m)
BBO	Biogeography-Based Optimization
C	heat capacity rate (W/K)
C_e	energy cost (€/kWh)
C_i	capital investment (€)
C_o	annual operating cost (€/yr)
Cod	total discounted operating cost (€)
C_p	specific heat (J/kg K)
CSA	Cuckoo Search Algorithm
C_{tot}	total annual cost (€)
D	dimension
d_e	hydraulic shell diameter (m)
d_i	tube inside diameter (m)
d_o	tube outside diameter (m)
D_s	shell internal diameter (m)
Dh	hydraulic diameter (m)
DE	Differential Evolution
dep_p	depredation percentile
f	friction coefficient
F	temperature difference correction factor
$F_{1,2}$	constants
FA	Firefly Algorithm
f_i	function to evaluate
G	mass flux velocity (kg/m ² s)
GA	Genetic Algorithm
GD	Generational distance
h	convective heat transfer coefficient (W/m ² K)
H_{ot}	annual operating time (h/yr)
HYPV	Hypervolume metric
i	annual discount rate (%)
ICA	Imperialist Competitive Algorithm
iter	iteration
$iter_{max}$	maximum number of iterations
j	Colburn factor
JADE	Adaptive Differential Evolution
k	thermal conductivity (W/m K)
L	heat exchanger length (m)/tube length (m)
lb	lower bound
m	mass flow rate (kg/s)
MODA	Multi-Objective Dragonfly Algorithm
MOGOA	Multi-Objective Grasshopper Optimization Algorithm
MOOOA	Multi-Objective Owl Optimization Algorithm
MS	Maximum spread
MSSA	Multi-Objective Salp Swarm Algorithm
n	cluster number/fin frequency/number of tube passes
n_1	numerical constant
NSGA – II	Non-dominated Sorting Genetic Algorithm, version II
NTU	number of transfer units
N_t	number of tubes
NP	Number of population members
num_{pp}	number of principal perches
num_{sp}	number of secondary perches
ny	equipment life (yr)
OF	objective fitness
OBL	Opposition-Based Learning
ONVG	Overall Non-dominated Vector Generation
OOA	Owl Optimization Algorithm
P	pressure (N/m ²)
PSO	Particle Swarm Optimization
P_p	pumping power (W)
Pr	Prandtl number
PSO	Particle Swarm Optimization
ΔP	pressure drop (Pa)
Q	heat duty (W)
q	number of objectives
Re	Reynolds number
Rf	fouling resistance (m ² K/W)
S	Optimal set of solutions
SA	Simulated Annealing
SP	Spacing
S_t	tube pitch (m)
t	fin thickness (m)
T	temperature (K)
ΔT_{LM}	logarithmic mean temperature difference (K)
U	overall heat transfer coefficient (W/m ² K)
ub	upper bound
$v_{1,2}$	velocity
v_i	ith hypercube
v	fluid velocity (m/s)
x	individual position
ε	effectiveness
μ	viscosity (N/m ² s)
ρ	density (kg/m ³)
η	overall pumping efficiency
i	inlet
iter	current iteration
min	minimum
max	maximum
o	outlet
s	shell side
t	tube side
w	wall
sort	sorted

unique thermal equipment which facilitate the exchange of thermal energy among various fluid streams [9]. The type of heat exchangers most studied in the literature are shell-and-tube and plate-fin heat. The first one, shell-and-tube heat exchangers, is widely used in industrial processes such as condensers in nuclear power stations, steam generator in water reactor plants under pressure and to feed water heaters among other alternative energy applications in ocean, thermal and geothermal areas. The second one, plate-fin heat exchangers, is also used in several industrial processes, especially in gas-to-gas applications in cryogenics, micro-turbines, automobiles, chemical process plants, naval and aerospace applications [10].

Shell-and-tube heat exchangers have already been investigated by

several authors using different optimization algorithms where some specific problems were preferably used for comparison reasons. For example, Caputo et al. [11] target the cost minimization of such device using GA reaching a reduction of 14.5% in the total annual cost in comparison to the original non-optimized solution. After, Patel & Rao [12] aimed the same problem adopting PSO achieving better results than the previous study, about 4.1%, for the total annual cost. Following these examples, Khalfe et al. [13] evaluated the case study based on Simulated Annealing (SA) and obtaining values 3.89% lower than the first optimized solution achieved previously [11]. Interesting to notice that in that last referred work some geometric ratio constraints were implemented trying to include in the search process criterion

related, for example, to the fouling suppression, flow distribution and potential tube vibration.

Two years after Khalife et al. [13], the same case study was investigated in the works of Hadidi et al. [14] and Hadidi & Nazari [15] where Imperialist Competitive Algorithm (ICA) reached better results than GA, and Biogeography-Based Optimization (BBO) achieved better results than PSO, respectively. Again, after a pair of years, Asadi et al. [16] applied the Cuckoo Search Algorithm (CSA) that obtained 13.5%, 10.5%, 12.3% and 5.8% of reduction in the total annual cost in comparison to approaches GA, PSO, ICA and BBO, previously presented in literature.

Recently, Mohanty [17] using Firefly Algorithm (FA) and Vasconcelos Segundo et al. [18] applying a variant of Differential Evolution (DE) investigated the same case study and the results outperformed the ones obtained by the previous works, with reductions 16.8% and 14.5% in comparison to GA, and 4% and 1.15% in comparison to CSA, respectively. Important to notice that the previous studies adopted decision variables for the optimization process that seek to balance the cost related to the heat exchanger area with the cost related to operational aspects. These peculiarities will be further explained in this present paper.

Some studies related to the optimization of more than one objective function for shell-and-tube heat exchangers can be found. Sanaye & Hajabdollahi [19] investigated shell-and-tube heat exchanger optimization considering the total cost and the efficiency as objective functions, a work further also studied by Ayala et al. [20]. Fettaka et al. [21] applied the Non-dominated Sorting Genetic Algorithm II (NSGA-II) considering the minimization of heat transfer area and pumping power. Ghanei et al. [22] implemented a multi-objective version of the Particle Swarm Optimization for the maximization of efficiency and the minimization of total cost of the system, where the results were compared to the reference method of NSGA-II. Recently Rao & Patel [23] performed a multi-objective optimization of shell-and-tube heat exchanger using a

modified teaching-learning-based optimization algorithm.

Similarly to the shell-and-tube heat exchanger, other topologies may also be greatly explored, as the plate fin heat exchangers for single [24–28] and multi-objective [29–34] and spiral heat exchangers for single [35–37] and multi-objective [36] optimization, where goals like minimization cost and entropy generations units and maximization effectiveness and rate of heat transfer were investigated.

The motivation of this work is to propose a novel population-based nature-inspired approach called Owl Optimization Algorithm (OOA) providing an adequate balance between exploration and exploitation behaviors competing with optimization algorithms to single-objective with few control parameters adjustment. The main inspiration of the OOA is the decoy behavior of the owls when any kind of danger is detected near the nests, when these animals performs back-and-forth movements between perches away from the nest to diverge potential predators. The no free lunch theorem also supports the motivation of this work to propose this optimizer since the OOA may outperform other algorithms on some problems that have not been solved so far. This theorem reveals the importance of new and specific algorithms in different fields because effectiveness of an algorithm in solving a set of problems does not guarantee its success in different sets of benchmark problems.

The remainder of this paper is organized as follows. Section 2 presents the decoy behavior of owls and its implementation procedure. After, Section 3 describes the experimental setup and analysis tools of performance. The results of the proposed OOA for several single-objective benchmark functions and engineering design problems are provided in Section 4, verifying the efficiency of the OOA. Finally, Section 5 concludes the work and suggests directions for future studies.

2. Owl optimization algorithm

The following subsections presents the inspiration of the algorithm

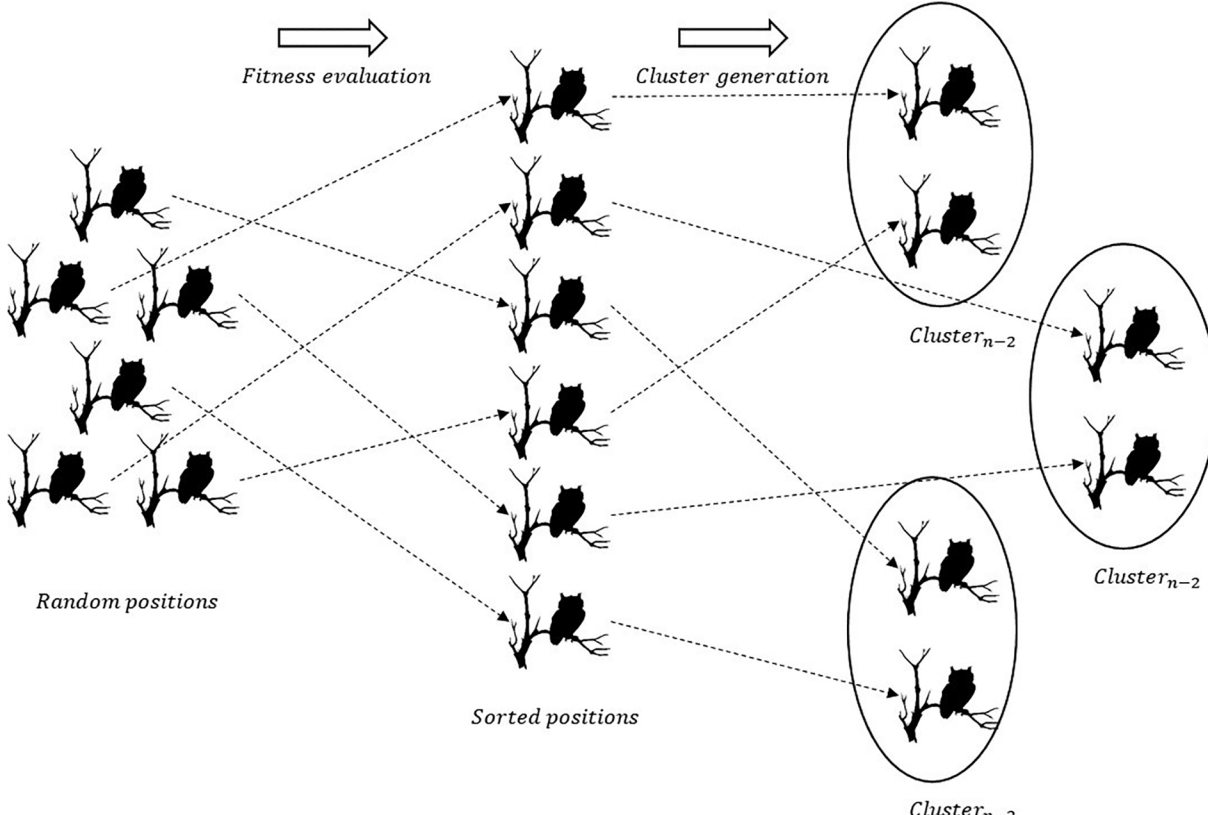


Fig. 1. Sorting and cluster generation for 1 principal perch e 1 secondary perch for 6 owls (performing 3 clusters).

and the steps adopted to its proper implementation.

2.1. Decoy behavior of owls

The inspiration of this algorithm was the decoy behavior of burrowing owls when a predator or any other kind of danger is near their nests. Owls are not fast animals, so it has to develop different strategies to avoid predator attacks. One of the most interesting facts about this animal consists in a part of its social behavior, the decoy behavior. If an owl is approached closely, it flies to one of a limited number of secondary perches, usually two, located near the burrow, or nest [36].

When the same burrow, or nest, is approached from different directions the owl flies to the same secondary perch. If the owl is pressed, it will circulate back and forth among the secondary perches. The owl uses this movement to divert a terrestrial predator, calling attention to itself through a ritualized pattern, and then retreats to a preferred perch [36]. The goal at this point is to prescind that the movement performed by the owl amongst the perches can be used for the search process in an optimization algorithm. Another interesting fact about this species is the nesting behavior where some percentage of the nests are depredated for the nest season [37].

2.2. Single-objective algorithm

The OOA has 5 control parameters to tune, num_{pp} , num_{sp} , dep_p , F_1 e F_2 , where the two last are random values generated with uniform distribution in range $[0, 1]$ and the first three values refer the cluster process and nest renewal.

Step 1: Initialize problem setup and adjustable control parameters

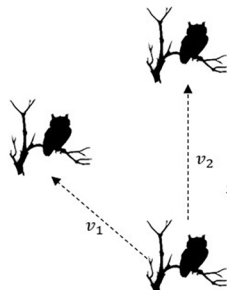
The optimization problem, decision variables and constraints, if they exist, are defined. Then, the adjustable parameters of OOA such as quantity of owls (NP), number of principal perches (num_{pp}), number of secondary perches (num_{sp}), maximum number of iterations ($iter_{max}$) and deprecated nests percentile (dep_p). It is important to notice that the quantity of owls must be consistent with the number of principal perches and secondary perches according to $NP = num_{pp} + num_{sp} num_{pp}$.

Step 2: Initialize position of the owls

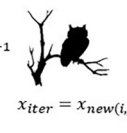
The owls are randomly positioned in a D -dimensional space respecting the boundary conditions, generating the matrix:

$$v_1 = F_1(x_{sort(i-num_{pp},j)} - x_{iter-1(i,j)})$$

$$v_2 = F_1(x_{sort(counter-1,j)} - x_{iter-1(i,j)})$$



OF_{iter} is better than OF_{iter-1}



$$x_{iter} = x_{new(i,j)}$$

OF_{iter} is not better than OF_{iter-1}



$$x_{iter} = x_{iter-1(i,j)}$$

$$x_{new(i,j)} = x_{iter-1(i,j)} + v_1 + v_2$$

$$v_1 = F_1(x_{sort(better,j)} - x_{iter-1(i,j)})$$

$$v_2 = F_1(x_{sort(1,j)} - x_{iter-1(i,j)})$$

$$v_1 = F_1(x_{sort(1,j)} - x_{iter-1(i,j)})$$

$$v_2 = F_1(x_{sort(1,j)} - x_{iter-1(i,j)})$$

$$v_1 = F_1(x_{sort(1,j)} - x_{iter-1(i,j)})$$

$$v_2 = F_1(x_{sort(1,j)} - x_{iter-1(i,j)})$$

$$v_1 = F_1(x_{sort(1,j)} - x_{iter-1(i,j)})$$

$$v_2 = F_1(x_{sort(1,j)} - x_{iter-1(i,j)})$$

$$v_1 = F_1(x_{sort(1,j)} - x_{iter-1(i,j)})$$

$$v_2 = F_1(x_{sort(1,j)} - x_{iter-1(i,j)})$$

$$v_1 = F_1(x_{sort(1,j)} - x_{iter-1(i,j)})$$

$$v_2 = F_1(x_{sort(1,j)} - x_{iter-1(i,j)})$$

$$v_1 = F_1(x_{sort(1,j)} - x_{iter-1(i,j)})$$

$$v_2 = F_1(x_{sort(1,j)} - x_{iter-1(i,j)})$$

$$v_1 = F_1(x_{sort(1,j)} - x_{iter-1(i,j)})$$

$$v_2 = F_1(x_{sort(1,j)} - x_{iter-1(i,j)})$$

$$v_1 = F_1(x_{sort(1,j)} - x_{iter-1(i,j)})$$

$$v_2 = F_1(x_{sort(1,j)} - x_{iter-1(i,j)})$$

$$v_1 = F_1(x_{sort(1,j)} - x_{iter-1(i,j)})$$

$$v_2 = F_1(x_{sort(1,j)} - x_{iter-1(i,j)})$$

$$v_1 = F_1(x_{sort(1,j)} - x_{iter-1(i,j)})$$

$$v_2 = F_1(x_{sort(1,j)} - x_{iter-1(i,j)})$$

$$v_1 = F_1(x_{sort(1,j)} - x_{iter-1(i,j)})$$

$$v_2 = F_1(x_{sort(1,j)} - x_{iter-1(i,j)})$$

$$v_1 = F_1(x_{sort(1,j)} - x_{iter-1(i,j)})$$

$$v_2 = F_1(x_{sort(1,j)} - x_{iter-1(i,j)})$$

$$v_1 = F_1(x_{sort(1,j)} - x_{iter-1(i,j)})$$

$$v_2 = F_1(x_{sort(1,j)} - x_{iter-1(i,j)})$$

$$v_1 = F_1(x_{sort(1,j)} - x_{iter-1(i,j)})$$

$$v_2 = F_1(x_{sort(1,j)} - x_{iter-1(i,j)})$$

$$v_1 = F_1(x_{sort(1,j)} - x_{iter-1(i,j)})$$

$$v_2 = F_1(x_{sort(1,j)} - x_{iter-1(i,j)})$$

$$v_1 = F_1(x_{sort(1,j)} - x_{iter-1(i,j)})$$

$$v_2 = F_1(x_{sort(1,j)} - x_{iter-1(i,j)})$$

$$v_1 = F_1(x_{sort(1,j)} - x_{iter-1(i,j)})$$

$$v_2 = F_1(x_{sort(1,j)} - x_{iter-1(i,j)})$$

$$v_1 = F_1(x_{sort(1,j)} - x_{iter-1(i,j)})$$

$$v_2 = F_1(x_{sort(1,j)} - x_{iter-1(i,j)})$$

$$v_1 = F_1(x_{sort(1,j)} - x_{iter-1(i,j)})$$

$$v_2 = F_1(x_{sort(1,j)} - x_{iter-1(i,j)})$$

$$v_1 = F_1(x_{sort(1,j)} - x_{iter-1(i,j)})$$

$$v_2 = F_1(x_{sort(1,j)} - x_{iter-1(i,j)})$$

$$v_1 = F_1(x_{sort(1,j)} - x_{iter-1(i,j)})$$

$$v_2 = F_1(x_{sort(1,j)} - x_{iter-1(i,j)})$$

$$v_1 = F_1(x_{sort(1,j)} - x_{iter-1(i,j)})$$

$$v_2 = F_1(x_{sort(1,j)} - x_{iter-1(i,j)})$$

$$v_1 = F_1(x_{sort(1,j)} - x_{iter-1(i,j)})$$

$$v_2 = F_1(x_{sort(1,j)} - x_{iter-1(i,j)})$$

$$v_1 = F_1(x_{sort(1,j)} - x_{iter-1(i,j)})$$

$$v_2 = F_1(x_{sort(1,j)} - x_{iter-1(i,j)})$$

$$v_1 = F_1(x_{sort(1,j)} - x_{iter-1(i,j)})$$

$$v_2 = F_1(x_{sort(1,j)} - x_{iter-1(i,j)})$$

$$v_1 = F_1(x_{sort(1,j)} - x_{iter-1(i,j)})$$

$$v_2 = F_1(x_{sort(1,j)} - x_{iter-1(i,j)})$$

$$v_1 = F_1(x_{sort(1,j)} - x_{iter-1(i,j)})$$

$$v_2 = F_1(x_{sort(1,j)} - x_{iter-1(i,j)})$$

$$v_1 = F_1(x_{sort(1,j)} - x_{iter-1(i,j)})$$

$$v_2 = F_1(x_{sort(1,j)} - x_{iter-1(i,j)})$$

$$v_1 = F_1(x_{sort(1,j)} - x_{iter-1(i,j)})$$

$$v_2 = F_1(x_{sort(1,j)} - x_{iter-1(i,j)})$$

$$v_1 = F_1(x_{sort(1,j)} - x_{iter-1(i,j)})$$

$$v_2 = F_1(x_{sort(1,j)} - x_{iter-1(i,j)})$$

$$v_1 = F_1(x_{sort(1,j)} - x_{iter-1(i,j)})$$

$$v_2 = F_1(x_{sort(1,j)} - x_{iter-1(i,j)})$$

$$v_1 = F_1(x_{sort(1,j)} - x_{iter-1(i,j)})$$

$$v_2 = F_1(x_{sort(1,j)} - x_{iter-1(i,j)})$$

$$v_1 = F_1(x_{sort(1,j)} - x_{iter-1(i,j)})$$

$$v_2 = F_1(x_{sort(1,j)} - x_{iter-1(i,j)})$$

$$v_1 = F_1(x_{sort(1,j)} - x_{iter-1(i,j)})$$

$$v_2 = F_1(x_{sort(1,j)} - x_{iter-1(i,j)})$$

$$v_1 = F_1(x_{sort(1,j)} - x_{iter-1(i,j)})$$

$$v_2 = F_1(x_{sort(1,j)} - x_{iter-1(i,j)})$$

$$v_1 = F_1(x_{sort(1,j)} - x_{iter-1(i,j)})$$

$$v_2 = F_1(x_{sort(1,j)} - x_{iter-1(i,j)})$$

$$v_1 = F_1(x_{sort(1,j)} - x_{iter-1(i,j)})$$

$$v_2 = F_1(x_{sort(1,j)} - x_{iter-1(i,j)})$$

$$v_1 = F_1(x_{sort(1,j)} - x_{iter-1(i,j)})$$

$$v_2 = F_1(x_{sort(1,j)} - x_{iter-1(i,j)})$$

$$v_1 = F_1(x_{sort(1,j)} - x_{iter-1(i,j)})$$

$$v_2 = F_1(x_{sort(1,j)} - x_{iter-1(i,j)})$$

$$v_1 = F_1(x_{sort(1,j)} - x_{iter-1(i,j)})$$

$$v_2 = F_1(x_{sort(1,j)} - x_{iter-1(i,j)})$$

$$v_1 = F_1(x_{sort(1,j)} - x_{iter-1(i,j)})$$

$$v_2 = F_1(x_{sort(1,j)} - x_{iter-1(i,j)})$$

$$v_1 = F_1(x_{sort(1,j)} - x_{iter-1(i,j)})$$

$$v_2 = F_1(x_{sort(1,j)} - x_{iter-1(i,j)})$$

$$v_1 = F_1(x_{sort(1,j)} - x_{iter-1(i,j)})$$

$$v_2 = F_1(x_{sort(1,j)} - x_{iter-1(i,j)})$$

$$v_1 = F_1(x_{sort(1,j)} - x_{iter-1(i,j)})$$

$$v_2 = F_1(x_{sort(1,j)} - x_{iter-1(i,j)})$$

$$v_1 = F_1(x_{sort(1,j)} - x_{iter-1(i,j)})$$

$$v_2 = F_1(x_{sort(1,j)} - x_{iter-1(i,j)})$$

$$v_1 = F_1(x_{sort(1,j)} - x_{iter-1(i,j)})$$

$$v_2 = F_1(x_{sort(1,j)} - x_{iter-1(i,j)})$$

$$v_1 = F_1(x_{sort(1,j)} - x_{iter-1(i,j)})$$

$$v_2 = F_1(x_{sort(1,j)} - x_{iter-1(i,j)})$$

$$v_1 = F_1(x_{sort(1,j)} - x_{iter-1(i,j)})$$

$$v_2 = F_1(x_{sort(1,j)} - x_{iter-1(i,j)})$$

$$v_1 = F_1(x_{sort(1,j)} - x_{iter-1(i,j)})$$

$$v_2 = F_1(x_{sort(1,j)} - x_{iter-1(i,j)})$$

$$v_1 = F_1(x_{sort(1,j)} - x_{iter-1(i,j)})$$

$$v_2 = F_1(x_{sort(1,j)} - x_{iter-1(i,j)})$$

$$v_1 = F_1(x_{sort(1,j)} - x_{iter-1(i,j)})$$

$$v_2 = F_1(x_{sort(1,j)} - x_{iter-1(i,j)})$$

$$v_1 = F_1(x_{sort(1,j)} - x_{iter-1(i,j)})$$

$$v_2 = F_1(x_{sort(1,j)} - x_{iter-1(i,j)})$$

$$v_1 = F_1(x_{sort(1,j)} - x_{iter-1(i,j)})$$

$$v_2 = F_1(x_{sort(1,j)} - x_{iter-1(i,j)})$$

$$v_1 = F_1(x_{sort(1,j)} - x_{iter-1(i,j)})$$

$$v_2 = F_1(x_{sort(1,j)} - x_{iter-1(i,j)})$$

$$v_1 = F_1(x_{sort(1,j)} - x_{iter-1(i,j)})$$

$$v_2 = F_1(x_{sort(1,j)} - x_{iter-1(i,j)})$$

$$v_1 = F_1(x_{sort(1,j)} - x_{iter-1(i,j)})$$

$$v_2 = F_1(x_{sort(1,j)} - x_{iter-1(i,j)})$$

$$v_1 = F_1(x_{sort(1,j)} - x_{iter-1(i,j)})$$

$$v_2 = F_1(x_{sort(1,j)} - x_{iter-1(i,j)})$$

$$v_1 = F_1(x_{sort(1,j)} - x_{iter-1(i,j)})$$

$$v_2 = F_1(x_{sort(1,j)} - x_{iter-1(i,j)})$$

$$v_1 = F_1(x_{sort(1,j)} - x_{iter-1(i,j)})$$

$$v_2 = F_1(x_{sort(1,j)} - x_{iter-1(i,j)})$$

$$v_1 = F_1(x_{sort(1,j)} - x_{iter-1(i,j)})$$

$$v_2 = F_1(x_{sort(1,j)} - x_{iter-1(i,j)})$$

$$v_1 = F_1(x_{sort(1,j)} - x_{iter-1(i,j)})$$

$$v_2 = F_1(x_{sort(1,j)} - x_{iter-1(i,j)})$$

$$v_1 = F_1(x_{sort(1,j)} - x_{iter-1(i,j)})$$

$$v_2 = F_1(x_{sort(1,j)} - x_{iter-1(i,j)})$$

$$v_1 = F_1(x_{sort(1,j)} - x_{iter-1(i,j)})$$

$$v_2 = F_1(x_{sort(1,j)} - x_{iter-1(i,j)})$$

$$v_1 = F_1(x_{sort(1,j)} - x_{iter-1(i,j)})$$

$$v_2 = F_1(x_{sort(1,j)} - x_{iter-1(i,j)})$$

$$v_1 = F_1(x_{sort(1,j)} - x_{iter-1(i,j)})$$

$$v_2 = F_1(x_{sort(1,j)} - x_{iter-1(i,j)})$$

$$v_1 = F_1(x_{sort(1,j)} - x_{iter-1(i,j)})$$

$$v_2 = F_1(x_{sort(1,j)} - x_{iter-1(i,j)})$$

$$v_1 = F_1(x_{sort(1,j)} - x_{iter-1(i,j)})$$

$$v_2 = F_1(x_{sort(1,j)} - x_{iter-1(i,j)})$$

$$v_1 = F_1(x_{sort(1,j)} - x_{iter-1(i,j)})$$

$$v_2 = F_1(x_{sort(1,j)} - x_{iter-1(i,j)})$$

$$v_1 = F_1(x_{sort(1,j)} - x_{iter-1(i,j)})$$

$$v_2 = F_1(x_{sort(1,j)} - x_{iter-1(i,j)})$$

$$v_1 = F_1(x_{sort(1,j)} - x_{iter-1(i,j)})$$

$$v_2 = F_1(x_{sort(1,j)} - x_{iter-1(i,j)})$$

$$v_1 = F_1(x_{sort(1,j)} - x_{iter-1(i,j)})$$

$$v_2 = F_1(x_{sort(1,j)} - x_{iter-1(i,j)})$$

$$v_1 = F_1(x_{sort(1,j)} - x_{iter-1(i,j)})$$

$$v_2 = F_1(x_{sort(1,j)} - x_{iter-1(i,j)})$$

$$v_1 = F_1(x_{sort(1,j)} - x_{iter-1(i,j)})$$

$$v_2 = F_1(x_{sort(1,j)} - x_{iter-1(i,j)})$$

$$v_1 = F_1(x_{sort(1,j)} - x_{iter-1(i,j)})$$

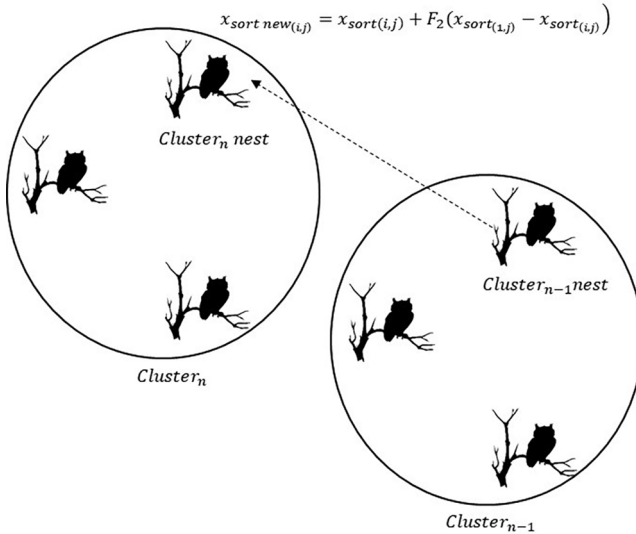


Fig. 3. Owl decoy behavior representation for the nest renovation.

Step 1. Initialize parameters:
 Population size, NP ;
 Maximum number of generations, $iter_{max}$;
 Quantity of primary perches, num_{pp} , secondary perches, num_{sp} , and depredated nests percentile, dep_p ;
 Insert boundaries restrictions ub , upper, and lb , lower bounds, and;
 Insert objective function.
Step 2. Initialization of the population with random positions.
Step 3. In $iter = 1$ for each individual calculate its corresponding OF .
 Generate $x_{sort} = sort(x)$ and $OF_{sort} = sort(OF)$.
 Generate random numbers F_1 and F_2 .
Step 4. for $iter = 2$ to $iter_{max}$ do:
Step 4.1. for $counter = 2$ to $(num_{pp} + 1)$ do:
 for $i = num_{pp} + (counter - 1):num_{pp}:num_{pp}num_{sp} + (counter - 1)$
 for $j = 1:D$
 $v_1 = F_1(x_{sort(i+num_{pp},j)} - x_{iter-1(i,j)})$
 $v_2 = F_1(x_{sort(counter-i,j)} - x_{iter-1(i,j)})$
 $x_{new(i,j)} = x_{iter-1(i,j)} + v_1 + v_2$
 end for
 Evaluate the fitness of each new individual;
 if $OF_{new} < OF_{iter-1}$
 $x_{iter(i,j)} = x_{new(i,j)}$
 else
 Select any better perch
 for $j = 1:D$
 $v_1 = F_1(x_{sort(better_i,j)} - x_{iter-1(i,j)})$
 $v_2 = F_1(x_{sort(i,j)} - x_{iter-1(i,j)})$
 $x_{new(i,j)} = x_{iter-1(i,j)} + v_1 + v_2$
 end for
 Evaluate the fitness of each new individual;
 if $OF_{new} < OF_{iter-1}$
 $x_{iter(i,j)} = x_{new(i,j)}$
 else
 $x_{iter(i,j)} = x_{iter-1(i,j)}$
 end if
 end for
Step 4.2. Renovate some nests according to the depredated percentile.
 for $i = 1$ to num_{pp}
 if $i > round(num_{pp}dep_p)$
 $x_{sort new(i,j)} = x_{sort(i,j)} + F_2(x_{sort(i,j)} - x_{sort(i,j)})$
 end if
 Evaluate the fitness of the new nest;
 if $OF_{sort new} < OF_{sort}$
 $x_{sort(i,j)} = x_{sort new(i,j)}$
 else
 $x_{sort(i,j)} = x_{sort(i,j)}$
 end if
 end for
Step 4.3. Update sorting;
 end for
Step 5. Output results.

Fig. 4. Pseudo code for the Owl Optimization Algorithm (OOA).

sorting process of the algorithm, for multi-objective optimization this procedure is performed for each iteration according to one of the objective functions, i.e., for example, for a bi-objective problem the first iteration performs the sorting according to the results for the first objective function, the second iteration according to the second and so on. This may be interpreted as the movement of the owl for the approaching of two predators where the animal tries to decoy at a time.

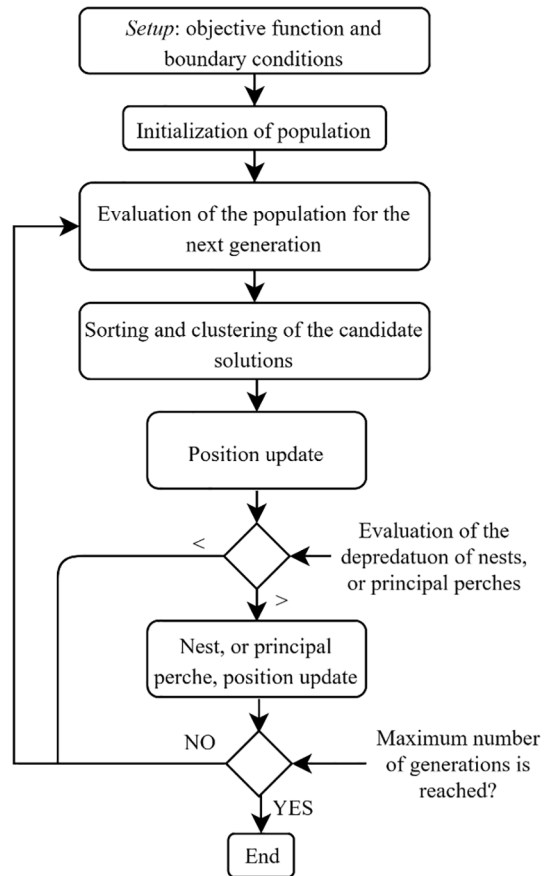


Fig. 5. Flowchart for the Owl Optimization Algorithm (OOA).

3. Experimental setup and analysis tools

It has been proved by no-free lunch theorem that no search algorithm is the best on average for all problems of optimization. An algorithm may solve some problems better and some problems worst in comparison to other algorithms. The evaluation of the optimization performance of the proposed OOA, and its multi-objective version, were made considering single and multiobjective benchmark functions with different natures and range of the decision variables. Owl Optimization Algorithm has been executed in the MATLAB® computational environment on a computer with i7-5500U 2.4 GHz processor with 16 GB RAM (Random Access Memory). The results and conclusions of the work are limited to the functions presented.

For single-objective benchmark optimization were performed 30 independent runs with an initial population of 30 individuals where OOA was set using 2 secondary perches and 10 principal perches, and maximum number of generations of 1000 which results were compared to GA and PSO. The multi-objective optimization evaluation of MOOOA consisted in the analysis of the results obtained with the ZDT1, ZDT2 and ZDT3 benchmark functions over 10 independent runs with an initial population of 50 candidates over 1000 generations and the results compared with NSGA-II [39], MSSA [40], MODA [41] and MOGOA [42]. For the engineering single-objective cases for heat exchanger optimization were adopted 30 independent runs with maximum number of iterations of 200 and $10D$ initial population for single-objective case studies (dependent to the number of decision variables of the problem), 10 principal perches and $D - 1$ secondary perches, and 100 initial population for the multi-objective case study.

3.1. Benchmark functions

The performance of the proposed OOA was evaluated considering ten well-known benchmark functions, seven for the single-objective optimization [43] and three for multi-objective optimization [44], presented by Table 1, respectively.

It is important to notice that Rastrigin is a continuous, differentiable, separable and scalable multimodal function while Griewank and Salomon functions resume the same characteristics, except separability. Sphere and Sum Squares are continuous, differentiable, separable and scalable unimodal functions, whilst Dixon & Price and Rotated Hyper-Ellipsoid keeps the same configuration considering that the first is not separable and the last is partially separable functions. Yet, ZDT1 is a convex function, ZDT2 is a concave function and ZDT3 presents a disconnected characteristic [45].

3.2. Shell-and-tube heat exchanger models and objective functions

The thermal modeling of the shell-and-tube heat exchangers case studies for single-objective optimization were taken from [11,18], originally taken from [46], where some adaptations considering content presented in Shah & Sekulic [10] were implemented.

Depending of the flow regime, the tube side heat transfer coefficient is calculated by,

$$h_t = \begin{cases} \left(\frac{k_t}{d_i}\right) \left[3.657 + \frac{0.0677 \left(Re_t Pr_t \left(\frac{d_i}{L}\right)\right)^{1.33}}{1 + 0.1 Pr_t \left(Re_t \left(\frac{d_i}{L}\right)\right)^{0.3}} \right], & Re_t \leq 2100 \\ \left(\frac{k_t}{d_i}\right) \left[\frac{\frac{f_t}{2} (Re_t - 1000) Pr_t}{1 + 12.7 \sqrt{\frac{f_t}{2} (Pr_t^{0.66} - 1)}} \right], & 2100 < Re_t < 10000 \\ 0.027 \left(\frac{k_t}{d_i}\right) Re_t^{0.8} Pr_t^{0.33} \left(\frac{\mu_t}{\mu_{wi}}\right)^{0.14}, & Re_t \geq 10000 \end{cases} \quad (3)$$

$$f_t = \begin{cases} (1.82 \log(Re_t) - 1.64)^{-2}, & Re_t \leq 2100 \\ 0.0054 + 0.00000023 \left(Re_t^{\frac{3}{2}}\right), & 2100 < Re_t < 4000 \\ 0.00128 + 0.1143 \left(Re_t^{\frac{-1}{3.214}}\right), & Re_t \geq 4000 \end{cases} \quad (4)$$

where k_t and f_t are the tube thermal conductivity and friction factor, respectively. The determination of h_t for $2100 < Re_t < 10000$, f_t for $2100 < Re_t < 4000$ and for $Re_t \geq 4000$. The Reynolds number is denoted by Re_t and can be computed by,

$$Re_t = \frac{\rho_t v_t d_i}{\mu_t} \quad (5)$$

The flow velocity for the tube side is given by,

$$v_t = \frac{\dot{m}_t}{\left(\frac{\pi}{4} d_i^2 \rho_t\right)} \left(\frac{n}{Nt}\right) \quad (6)$$

where n is the number of tube passes, d_i is the tube inside diameter ($d_i = 0.8d_o$) and Nt is the number of tubes, determined by,

$$Nt = K_1 \left(\frac{D_s}{d_o}\right)^{n_1} \quad (7)$$

Table 1
Benchmark test functions for single and multi-objective optimization.

Single-objective optimization benchmarks			
	Test function	Search space [lb, ub] ^D	Optimal value
Sphere	$f_1 = \sum_{i=1}^D x_i^2$	$[-100, 100]^30$	0
Griewank	$f_2 = \sum_{i=1}^D \frac{x_i^2}{4000} - \prod_{i=1}^D \cos\left(\frac{x_i}{\sqrt{i}}\right) + 1$	$[-600, 600]^30$	0
Rastrigin	$f_3 = 10D + \sum_{i=1}^D [x_i^2 - 10\cos(2\pi x_i)]$	$[-5.12, 5.12]^30$	0
Rotated Hyper-Ellipsoid	$f_4 = \sum_{i=1}^D \sum_{j=1}^i x_j^2$	$[-65, 65]^30$	0
Dixon & Price	$f_5 = (x_1 - 1)^2 + \sum_{i=1}^D i(2x_i^2 - x_{i-1})^2$	$[-10, 10]^30$	0
Salomon	$f_6 = -\cos\left(2\pi \sqrt{\sum_{i=1}^D x_i^2}\right) + 0.1 \sqrt{\sum_{i=1}^D x_i^2} + 1$	$[-100, 100]^30$	0
Sum of Squares	$f_7 = \sum_{i=1}^D i x_i^2$	$[-5.12, 5.12]^30$	0
Multi-objective optimization benchmarks			
	Test function	Search space [lb, ub] ^D	
ZDT1	$f_1 = x_1; f_2 = g(x) \left[1 - \sqrt{\frac{x_1}{g(x)}} \right]$	$[0, 1]^{10}$	
ZDT2	$f_1 = x_1; f_2 = g(x) \left[\frac{f_1}{g(x)} \right]^2$	$[0, 1]^{10}$	
ZDT3	$f_1 = x_1; f_2 = g(x) \left[1 - \sqrt{\frac{f_1}{g(x)}} - \sin(10\pi f_1) \left(\frac{f_1}{g(x)}\right) \right]$ where $g(x) = 1 + 9 \left(\frac{\sum_{i=2}^n x_i}{n-1} \right)$	$[0, 1]^{10}$	

Notation: lb means lower bound, ub means upper bound and D is the dimension of the function.

where K_1 and n_1 are coefficients determined based on the flow arrangement, triangular pitch on the case of this work, and number of passes.

The tube side Prandtl number is determined by,

$$Pr_t = \frac{\mu_t C p_t}{k_t} \quad (8)$$

The shell side heat transfer coefficient is given as,

$$h_s = 0.36 \left(\frac{k_s}{de} \right) Re_s^{0.55} Pr_s^{0.33} \left(\frac{\mu_s}{\mu_{ws}} \right)^{0.14} \quad (9)$$

where de is the shell hydraulic diameter, or equivalent diameter, given as

$$de = \frac{4 \left(0.43 St^2 - \left(\frac{0.5 \pi d_o^2}{4} \right) \right)}{0.5 \pi d_o} \quad (10)$$

$$St = 1.25 d_o$$

The Prandtl number for the shell side is given by,

$$Pr_s = \frac{\mu_s C p_s}{k_s} \quad (11)$$

The flow velocity for the shell side is determined by,

$$v_s = \frac{\dot{m}_s}{\rho_s A_s} \quad (12)$$

where A_s is the cross-sectional area normal to flow direction given by,

$$A_s = D_s B \left(1 - \frac{d_o}{St} \right) \quad (13)$$

The Reynolds number for the shell side is obtained from,

$$Re_s = \frac{\dot{m}_s de}{A_s \mu_s} \quad (14)$$

The overall heat transfer coefficient can be determined by,

$$U = \frac{1}{\frac{1}{h_s} + Rf_s + \left(\frac{d_o}{d_i} \right) \left(Rf_t + \frac{1}{h_t} \right)} \quad (15)$$

The logarithmic mean temperature is obtained from,

$$\Delta T_{LM} = \frac{(T_{hi} - T_{co}) - (T_{ho} - T_{ci})}{\ln \left(\frac{T_{hi} - T_{co}}{T_{co} - T_{ci}} \right)} \quad (16)$$

The correction factor is given by,

$$F = \sqrt{\frac{R^2 + 1}{R - 1}} \frac{\ln \left(\frac{1 - P}{1 - PR} \right)}{\ln \left(\frac{2 - PR + 1 - \sqrt{R^2 + 1}}{2 - PR + 1 + \sqrt{R^2 + 1}} \right)} \quad (17)$$

where R , the correction coefficient, and P , the efficiency, are determined respectively by,

$$R = \frac{T_{hi} - T_{ho}}{T_{co} - T_{ci}} \quad (18)$$

$$P = \frac{T_{co} - T_{ci}}{T_{hi} - T_{ci}} \quad (19)$$

The heat exchanger surface area is given by,

$$A = \frac{Q}{UFh T_{LM}} \quad (20)$$

For sensible heat transfer, the rate of heat transfer is determined by,

$$Q = \dot{m}_h C p_h (T_{hi} - T_{ho}) = \dot{m}_c C p_c (T_{co} - T_{ci}) \quad (21)$$

The tube length is obtained from,

$$L = \frac{A}{\pi d_o N_t} \quad (22)$$

The tube side pressure drop is computed as the sum of the distributed pressure drop along the tube length and concentrated pressure losses in elbows as well as in the inlet and outlet nozzles,

$$\Delta P_t = \frac{\rho_t v_t^2}{2} \left(\frac{L}{d_i} f_t + 4 \right) n \quad (23)$$

The shell side pressure drop is,

$$\Delta P_s = 1.44 Re_s^{-0.15} \left[\left(\frac{\rho_s v_s^2}{2} \right) \left(\frac{L}{B} \right) \left(\frac{D_s}{de} \right) \right] \quad (24)$$

where f_t is the friction factor.

For the multi-objective optimization case study the model presented in [19] were implemented, where number of transfer units is given by,

$$NTU = \frac{UA_t}{C_{min}} \quad (25)$$

where the overall heat transfer coefficient is obtained applying,

$$U = \frac{1}{\frac{1}{h_s} + Rf_s + \frac{d_o \ln \left(\frac{d_o}{d_i} \right)}{2k_w} + \frac{Rf_t d_o}{d_i} + \frac{1}{h_t} \frac{d_o}{d_i}} \quad (26)$$

where k_w is the thermal conductivity of the tube wall and the total tube outside heat transfer surface area is,

$$A_t = \pi L d_o N_t \quad (27)$$

For the tube side, the heat transfer coefficient for $2500 < Re_t < 1.24 \times 10^5$ is calculated using,

$$h_t = \left(\frac{k_t}{d_i} \right) 0.024 Re_t^{0.8} Pr_t^{0.4} \quad (28)$$

where the Reynolds number is given by,

$$Re_t = \frac{m_t d_i}{\mu_t A_{ot}} \quad (29)$$

in which the tube side flow cross section area per pass is estimated as,

$$A_{ot} = \frac{0.25 \pi d_i^2 N_t}{np} \quad (30)$$

For the multi-objective optimization heat exchanger model, the pressure drop is estimated as,

$$\Delta P_t = \frac{G^2}{2 \rho_i} \left[(1 - \sigma^2 + Kc) + 2 \left(\frac{\rho_i}{\rho_o} - 1 \right) + \frac{4 f_t L}{d_i} \rho_i \left(\frac{1}{\rho} \right)_m - \frac{(1 - \sigma^2 - Ke) \rho_i}{\rho_o} \right] \quad (31)$$

where is included the pressure drop due to flow contraction, acceleration, friction and expansion, and Kc and Ke are the tube entrance and exit pressure loss coefficients, with friction coefficient obtained by the relation $f_t = 0.00128 + 0.1143 Re_t^{-0.311}$ for Reynolds number between 4000 and 10^7 .

About the shell side, the shell diameter is obtained by,

$$D_s = 0.637 S_t \sqrt{\frac{\pi N_t CL}{CTP}} \quad (32)$$

where CL is tube layout constant that has a unit value for 45° and 90° tube arrangement and 0.87 for 30° and 60° tube arrangement, and CTP is tube count constant which is 0.93, 0.9 and 0.85 for single pass, two passes and three passes respectively.

Yet, the Bell-Delaware method was considered regarding the shell side heat transfer coefficient,

$$h_s = j_s c p_s \left(\frac{m_s}{A_s} \right) \left(\frac{k_s}{c p_s \mu_s} \right)^{\frac{2}{3}} \left(\frac{\mu_s}{\mu_{s,w}} \right)^{0.14} J_c J_t J_b J_s J_r \quad (33)$$

where j_s is the ideal tube bank Culburn factor and $\left(\frac{\mu_s}{\mu_{s,w}} \right)$ is the viscosity ratio at bulk to wall temperature in the shell side.

And the pressure drop for the shell side, computing the crossflow pressure drop, inlet and outlet pressure drop and windows section pressure drop respectively, is determined by,

$$\Delta P_s = \Delta P_{cr} + \Delta P_{l-o} + \Delta P_w \quad (34)$$

where details of how to compute all these terms can be found in [47].

The objective function for the total annual cost includes capital investment (C_i), energy cost (C_e), annual operating cost (C_o), and the total discounted operating cost (Cod).

$$C_{tot} = C_i + C_{od} \quad (35)$$

The capital investment cost is determined as a function of the heat exchanger surface area according to Hall's correlation [48],

$$C_i = a_1 + a_2 A^{a_3} \quad (36)$$

where a_1 , a_2 and a_3 are constants with dependency of the material of the heat exchanger.

The total discounted operating cost is determined as a function of the pressure drops for shell and tube sides as,

$$C_{od} = \sum_{j=1}^{ny} \frac{C_o}{(1+i)^j} \quad (37)$$

$$C_o = P_p C e H_{ot} \quad (38)$$

$$P_p = \frac{1}{\eta} \left(\frac{\dot{m}_t}{\rho_t} \Delta P_t + \frac{\dot{m}_s}{\rho_s} \Delta P_s \right) \quad (39)$$

where C_e is the energy cost, H_{ot} is the annual operating time, i is the annual discount rate and η is the overall pumping efficiency.

Also, the efficiency for the shell-and-tube heat exchanger is given by [19]

$$\varepsilon = \frac{2}{\left\{ (1+C) + (1+C^2)^{0.5} \coth \left[\frac{NTU}{2} (1+C^2)^{0.5} \right] \right\}} \quad (40)$$

where C is the heat capacity ratio $\left(\frac{C_{min}}{C_{max}} \right)$, and NTU the number of transfer units.

3.3. Analysis tools

The performance of the single-objective optimization considered not only convergence and best fitness value obtained, but also computational processing time and average fitness value during the generations.

Multiobjective performance analysis consists, normally, about the evaluation of capacity, convergence and diversity [49]. The multi-objective evaluation of performance considered the metrics called Overall Non-dominated Vector Generation (ONVG) for capacity, Generational Distance (GD) for convergence evaluation and Spacing (SP) and Maximum Spread (MS) for diversity evaluation, alongside with Hypervolume indicator (HV) for convergence-diversity.

The capacity metric of ONVG accounts the amount of non-dominated points presented in the Pareto Front [50], given by

$$ONVG(S) = |S| \quad (41)$$

where $|S|$ defines the cardinality, i.e., the amount of non-dominated elements presented in the Pareto Front.

Convergence metrics is about measuring the degree of proximity based on the distance between the solution in S to those in the true Pareto Front [49]. The Generational Distance (GD) metric [51] is given by:

$$GD(S, P) = \frac{\left(\sum_{i=1}^{|S|} d_i^q \right)^{\frac{1}{q}}}{|S|} \quad (42)$$

where d_i is the smallest distance between the Pareto set to the closest solution in P and q is the number of objectives. Here the Euclidian distance is applied, unless explicitly indicated.

Diversity metrics indicate the distribution and spread of solutions in the optimal set (S). The Spacing (SP) metric [49] is given by:

$$SP = \sqrt{\frac{\sum_{i=1}^{|S|} (d_i - d)^2}{(|S| - 1)}} \quad (43)$$

where d_i is the smallest distance between the Pareto set to the closest solution in the optimal set S . Here, again, the Euclidian distance is applied, unless explicitly indicated. Also about diversity, the metrics of Maximum Spread defines the Euclidian distance in relation to the maximum values obtained for each objective evaluated.

The convergence-diversity metric measured the quality of the optimal solution set S in terms of convergence and diversity on a single scale [49]. One of the most commonly used metrics are the Hypervolume (HYPV) [52] given by:

$$HYPV(S) = \text{volume} \left(\bigcup_{i=1}^{|S|} v_i \right) \quad (44)$$

where the Hypervolume is the are given by the enclosed discontinuous boundary given for each feasible solution, being that for each solution in S a hypercube v_i is constructed with the reference set and the solution as the diagonal corners of the hypercube.

4. Results and discussion

The next subsections present the results for the benchmark functions and for the engineering cases for both heat exchangers typologies optimization.

4.1. Benchmark functions results

The performance of the single-objective optimization considered not only convergence and best fitness value obtained, but also computational processing time. Also, an evaluation about direct comparison between the proposed algorithm and the reference techniques was performed using the Wilcoxon ranksum test.

The setup parameters for the comparison algorithms were: GA (crossover and mutation probabilities equal to 0.9 and 0.001, respectively) and PSO (cognitive and social constants equal to 2 and inertia weight equal to 0.5). For better understanding of the comparison algorithms, GA and PSO, the authors suggest consulting the references [4,6], respectively. Many versions of PSO and GA have been developed over the last 30 years. We compare the results of the proposed approach with that proposed in [53,54].

The results for the single-objective optimization best values are shown in Table 2 alongside to its mean and standard deviations values and comparison with GA and PSO.

It can be observed the OOA presented better results compared to GA and PSO in all seven benchmark functions tested, also presenting better mean values in six (except for f_7) and lower standard deviation in four of them (f_1 , f_3 , f_5 and f_6). The average processing time shows that the algorithm overcomes GA and PSO. The Wilcoxon ranksum test demonstrated that the for all of the simulations were statistically different. Fig. 6 presents the convergence rate for the fitness values during the generations. The convergence analysis of the fitness values also presents that the OOA did not suffered from stagnation in the searching process for any function tested. For better illustration of the search process the Fig. 7 has been generate for the functions f_2 , f_3 , f_5 and f_6 (with $D = 2$ over 100 generations), where it can be seen that the population of OOA converges entirely to the global optimal point.

Table 2

Results obtained for OOA in comparison to GA and PSO for the single-objective benchmark functions (best results in bold font) and *p*-values of the Wilcoxon ranksum test over all runs for direct comparison between OOA and the other techniques.

	Best	Avg.	Std.	Avg. time (s)	<i>p</i> -values for the Wilcoxon ranksum test
f_1	GA	2.4142E+00	4.7844E+00	1.9540E+00	0.6005
	PSO	3.4187E+00	1.1950E+01	5.3295E+00	5.7375
	OOA	0.0000E+00	0.0000E+00	0.0000E+00	0.4313
f_2	GA	9.9682E-01	1.0459E+00	1.6182E-02	0.6250
	PSO	1.0533E+00	1.0983E+00	3.8037E-02	5.8734
	OOA	0.0000E+00	3.6817E-02	2.0166E-01	0.5323
f_3	GA	2.0587E+01	3.6659E+01	9.9996E+00	0.5911
	PSO	2.1017E+01	4.1164E+01	1.3662E+01	5.8557
	OOA	0.0000E+00	2.7897E-01	1.5280E+00	0.3870
f_4	GA	1.1079E+01	2.5409E+01	8.2967E+00	0.8750
	PSO	2.3925E+01	5.6466E+01	2.6648E+01	6.0359
	OOA	0.0000E+00	3.9531E+00	2.1652E+01	0.6182
f_5	GA	1.6216E+00	4.3832E+00	2.0198E+00	0.5797
	PSO	2.1654E+00	4.5850E+00	1.5788E+00	5.7682
	OOA	0.0000E+00	2.3194E-01	1.2704E+00	0.2620
f_6	GA	1.6926E+01	2.2598E+01	3.2763E+00	0.6281
	PSO	2.3297E+01	2.8980E+01	4.1177E+00	5.9719
	OOA	0.0000E+00	1.1762E-01	6.4425E-01	0.5776
f_7	GA	8.6169E-02	1.5570E-01	4.5285E-02	0.5385
	PSO	1.4933E-01	3.7101E-01	1.2606E-01	5.7349
	OOA	0.0000E+00	4.1973E-01	2.2989E+00	0.3526

About the multi-objective optimization, the results for the ZDT1, ZDT2 and ZDT3 functions are presented in [Table 3](#) and [Fig. 8](#). Considering first the processing time, MOOOA presented lower time requirement than MODA and MOGOA.

From [Table 3](#) it can be observed that for the non-dominated points for all the trials performed with each algorithm MOOOA presented best capacity generation for ZDT1 and 2 and reached the second-best capacity generation for ZDT3. Also, the proposed algorithm obtained best convergence metric for ZDT2 and 3, keeping the second-best convergence value for ZDT1. Although about the diversity metric of Spacing best results weren't obtained, MOOOA reached the fourth position for ZDT1 and the third for ZDT2 and 3. For the Maximum Spread the results reveals that the multi-objective version of OOA reached the fourth position for ZDT1 and ZDT3 and the worst results for ZDT2. Considering the metric of quality for convergence-diversity, MOOOA presented the worst values for ZDT1 and ZDT2, but the second best for ZDT3. Probably the worst results obtained by the proposed technique regarding the Hypervolume is due to the poor distribution of the feasible Pareto points over the true Pareto Front.

4.2. Shell-and-tube heat exchangers optimization results

The following subsections presents the results obtained for the shell-and-tube heat exchangers case studies and their discussion.

The case study 1 for a shell-and-tube heat exchanger consists in the application by Sinnott et al. [\[46\]](#) where a heat exchanger with two tube passages and one shell passage between methanol and brackish water with a requirement heat duty of 4.43 MW needs to be designed for minimum total cost. The second one, from Kern [\[55\]](#), presents a heat exchanger with two tube passages and one shell passage between distilled water and raw water with a requirement heat duty of 0.46 MW

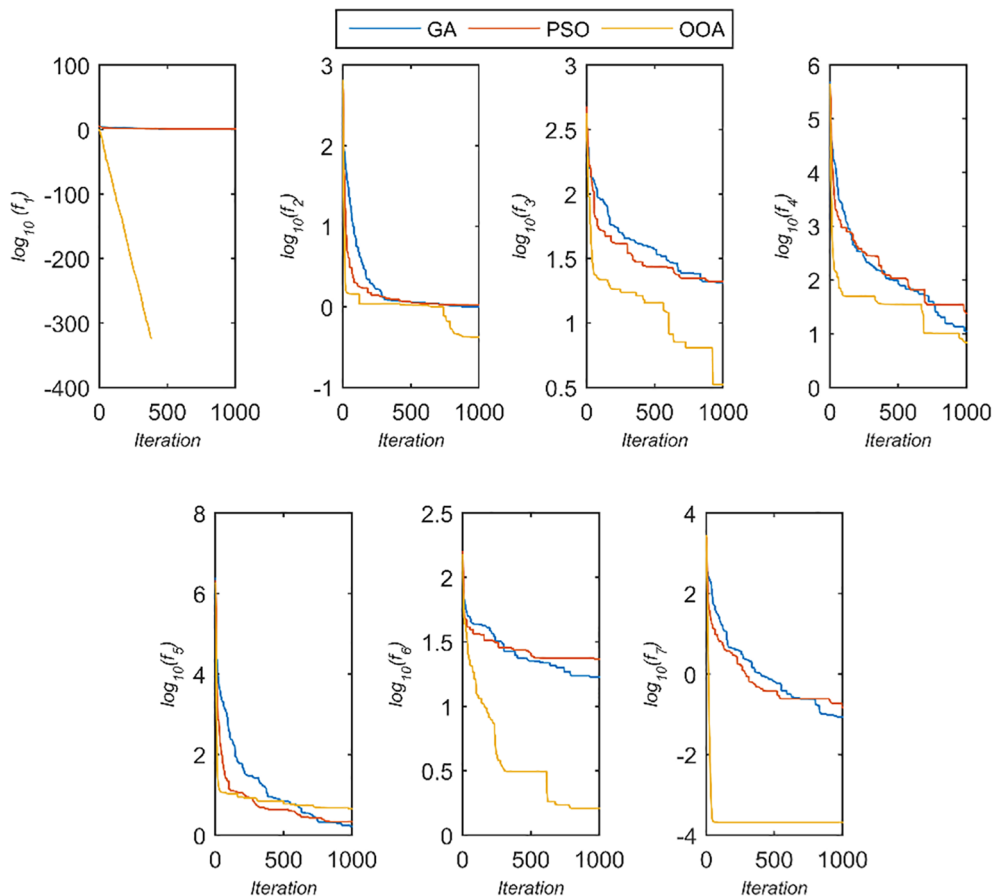


Fig. 6. Convergence rate for Sphere (f_1), Griewank (f_2), Rastrigin (f_3), Rotated Hyper-Ellipsoid (f_4), Dixon & Price (f_5), Salomon (f_6) and Sum of Squares functions (f_7).

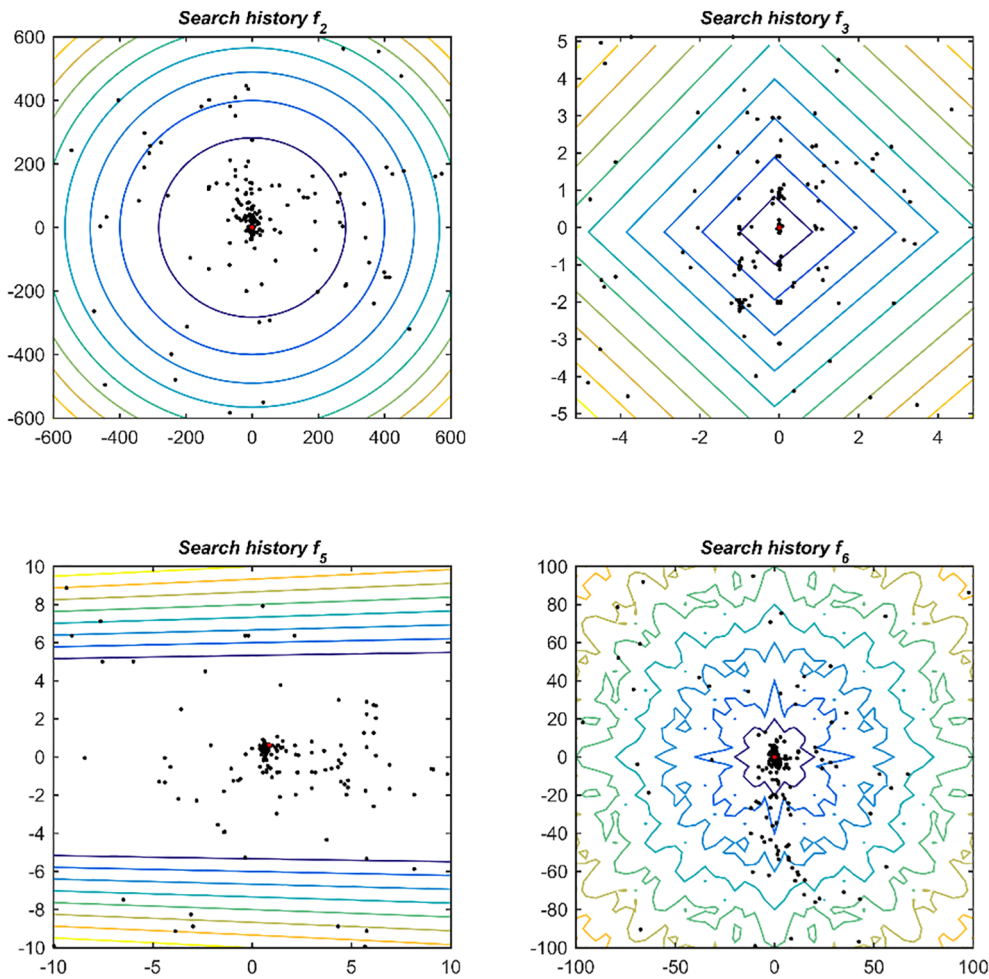


Fig. 7. Search history for Griewank function (f_2), Rastrigin function (f_3), Dixon & Price function (f_5) and Salomon function (f_6) over the 100 generations for $D = 2$.

Table 3

Results obtained for MOOOA in comparison to NSGA-II, MSSA, MODA and MOGOA for the quality metrics of capacity (ONVG), convergence (GD), diversity (SP and MS) and convergence-diversity (HYPV), where the best results are presented in bold font.

		ONVG↑	GD↓	SP↓	MS↑	HYPV↑
ZDT1	NSGA-II	270	4,69E-03	1,61E-02	2,14E+00	6,62E-01
	MSSA	201	5,85E-04	5,24E-03	9,77E-01	6,10E-01
	MODA	188	3,02E-04	3,37E-02	1,11E+00	6,02E-01
	MOGOA	243	1,25E-03	1,35E-03	1,12E+00	6,05E-01
	MOOOA	364	3,66E-04	2,78E-02	1,09E+00	5,80E-01
ZDT2	NSGA-II	336	7,93E-05	2,76E-03	1,41E+00	3,30E-01
	MSSA	266	4,18E-04	4,19E-03	9,46E-01	3,06E-01
	MODA	270	1,58E-03	2,88E-02	1,70E+00	3,15E-01
	MOGOA	253	6,43E-05	1,92E-03	1,18E+00	3,04E-01
	MOOOA	476	2,41E-05	3,02E-03	8,29E-01	2,46E-01
ZDT3	NSGA-II	384	9,15E-05	2,44E-03	1,97E+00	7,80E-01
	MSSA	238	9,52E-04	3,31E-03	1,49E+00	7,21E-01
	MODA	25	4,19E-02	2,04E-01	2,07E+00	5,79E-01
	MOGOA	138	7,33E-03	1,75E-02	2,03E+00	6,90E-01
	MOOOA	313	8,90E-05	4,79E-03	1,96E+00	7,78E-01

The symbols ↓ and ↑ represent “lower value better” and “higher value better” for ease understanding of the quality metrics.

that needs a design for minimum total cost.

For both case studies for single-objective optimization the constants for the investment cost were $a_1 = 8000$, $a_2 = 259.2$, and $a_3 = 0.91$ for heat exchangers made with stainless steel for shell and tubes, and for the operational cost, $C_e = 0.00012$, $H_{ot} = 7000$, $i = 0.1$, and $\eta = 0.8$.

Also, the coefficients for the determination of the number of tubes are $K_1 = 0.249$ and $n_1 = 2.207$ for triangular pitch in both cases. The lower and upper bounds of design variables adopted for both case studies were: the shell internal diameter (D_s) ranging from 0.1 m to 1.5 m; the tubes outside diameter (d_o) ranging from 0.008 m to 0.051 m and baffles spacing (B) ranging from 0.05 m to 0.50 m. The objective function was computed for the total discounted operating costs with $ny = 10$ years.

The multi-objective optimization shell-and-tube case study [19], the third case, consists in an oil cooler shell and tube heat recovery heat exchanger in Sarchesmeh copper production power plant located in south of Kerman city need to be optimized to maximize effectiveness and minimum total cost. The oil mass flowrate was 8.1 kg/s with 78.3 °C inlet temperature entered the shell side and the cold water flowrate was 12.5 kg/s at 30 °C entered the tube side. In this study the life period of the equipment was $ny = 10$ yr, the rate of annual discount was $i = 10\%$, the price of electricity was $k_{el} = 0.15 \frac{\$}{kWh}$, hours of operation $\tau = 7500 \frac{h}{yr}$ and pump efficiency was $\eta = 0.6$. Tube diameter (di) ranging from 0.0112 to 0.0153 m, number of tubes (N_t) ranging from 100 to 600, length of tubes (L) ranging from 3 to 8 m, tube pitch ratio ($\frac{pt}{do}$) ranging from 1.25 to 2 m, baffle cut ratio ($\frac{bc}{Ds}$) ranging from 0.19 to 0.32, baffle spacing ratio ($\frac{bc}{Ds}$) ranging from 0.2 to 1.4, number of tube passes (ntp) – 1, 2 or 3 passes – and tube arrangement (t_α) of 30°, 45° or 90° were considered as decision variables. The parameters inputs and physical properties of the fluids are presented in Table 4 for all case studies.

The results for the first case study, minimizing the total cost of the

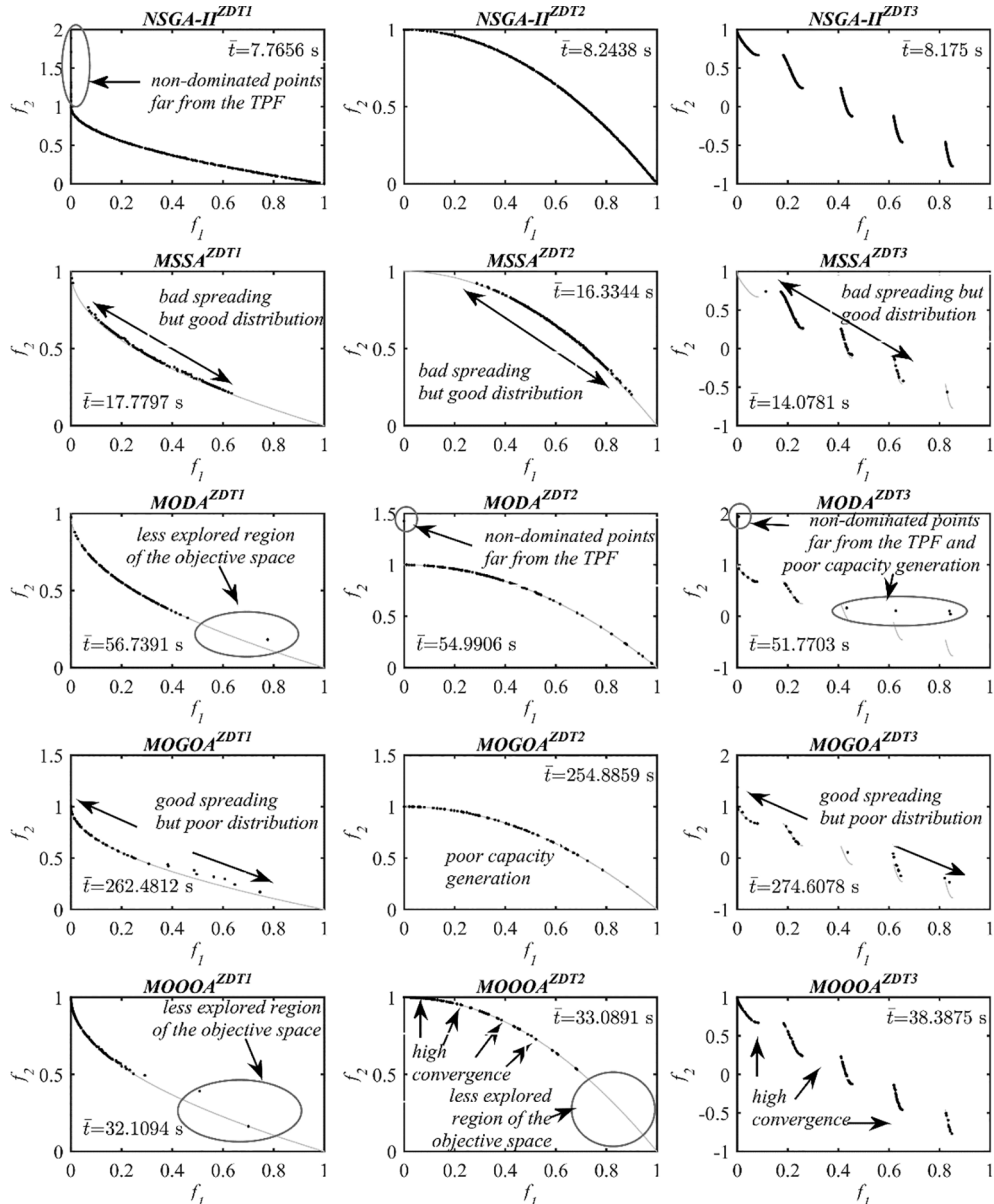


Fig. 8. Results for the ZDT1, ZDT2 and ZDT3 benchmark function for all the non-dominated point runs performed with each comparison algorithm (NSGA-II, MSSA, MODA and MOGOA) and for the MOOOA technique. Inside each plot is displayed the average processing time (\bar{t}) and pertinent comments about the quality metrics evaluation.

heat exchanger were compared with the works of Sinnott et al. [46], Caputo [11] (GA), Patel & Rao [12] (PSO), Khalife et al. [13] (SA), Hadidi et al. [14] (ICA), Hadidi & Nazari [15] (BBO) and Asadi et al.

[16] (CSA). The convergence of the best simulation obtained with OOA reached low variation under 50 iterations (Fig. 9(a)) and the comparison for the results obtained are presented in Table 5. It can be observed

Table 4
Shell-and-tube heat exchanger design specifications.

	Case 1		Case 2		Case 3	
	Shell side	Tube side	Shell side	Tube side	Shell side	Tube side
\dot{m} (kg/s)	27.80	68.90	22.07	35.31	8.1	12.5
T_i (°C)	95	25	33.9	23.9	78.3	30
T_o (°C)	40	40	29.4	26.7	—	—
ρ (kg/m ³)	750	995	995	995	860	995
C_p (kJ/kg.K)	2.84	4.20	4.18	4.18	2115	4120
μ (Pa.s)	0.00034	0.0008	0.0008	0.00092	0.0643	0.000695
μ_w (Pa.s)	0.00038	0.00052	—	—	—	—
k (W/m.K)	0.19	0.59	0.62	0.62	0.14	0.634
R_f (m ² K/W)	0.00033	0.0002	0.00017	0.00017	0.00015	0.000074

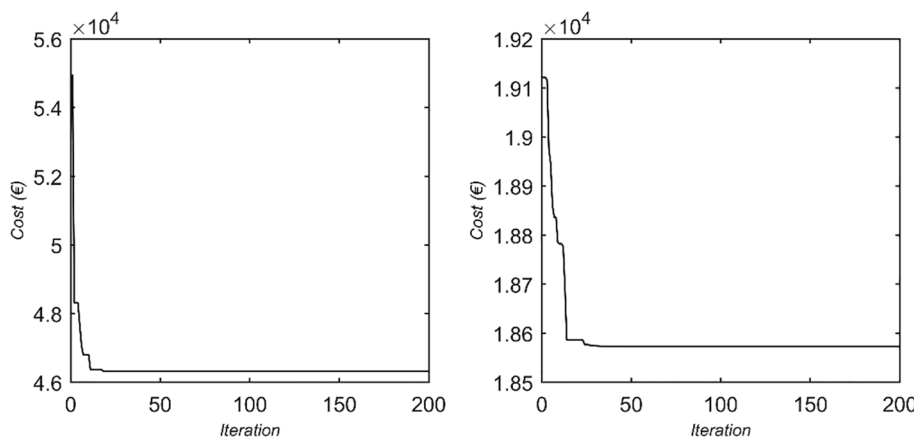


Fig. 9. Convergence curves for the shell-and-tube heat exchanger case study 1(a) and 2(b).

Table 5

Main geometrical and physical results for the optimum shell-and-tube heat exchanger configuration for first case study.

	Original design [46]	GA [11]	PSO [12]	SA [13]	ICA [14]	BBO [15]	CSA [16]	OOA
D _s (m)	0.894	0.830	0.810	0.740	0.879	0.801	0.826	0.825
L (m)	4.830	3.379	3.115	2.438	3.107	2.040	2.332	2.274
B (m)	0.356	0.500	0.424	–	0.500	0.500	0.414	0.492
d _o (m)	0.020	0.016	0.015	0.0095	0.015	0.010	0.0151	0.0144
N _t	918	1567	1658	3031	1658	3587	1754	2538
v _f (m/s)	0.75	0.69	0.67	1.00	0.699	0.77	0.65	0.93
R _{e_f}	14,925	10,936	10,503	–	10,429	7643	10,031	10,000
P _{r_f}	5.7	5.7	5.7	–	5.7	5.7	5.7	5.7
h _t (W/m ² K)	3812	3762	3721	5428.64	3864	4314	6104	9890
ΔP _t (Pa)	6251	4298	4171	12690.22	5122	6156	4186	5203
d _e (m)	0.014	0.011	0.0107	–	0.011	0.007	0.0107	0.0067
v _s (m/s)	0.58	0.44	0.53	0.42	0.42	0.46	0.56	0.52
R _{e_s}	18,381	11,075	12,678	–	9917	7254	13,716	7805
P _{r_s}	5.1	5.1	5.1	–	5.1	5.1	5.1	5.1
h _s (W/m ² K)	1573	1740	1950.8	2137.09	1740	2197	2083	2373
ΔP _s (Pa)	35,789	13,267	20,551	11708.97	12,367	13,799	22,534	18,483
U (W/m ² K)	615	660	713.9	–	677	755	848.2	886.6
A (m ²)	278.6	262.8	243.2	221.07	256.6	229.95	209.1	195.87
C _i (€)	51,507	49,259	46,453	43250.34	48,370	44,536	40343.70	39574.13
C _{od} (€)	12,973	5818	6778.2	9679.63	5995	6046	7281.40	6744.64
C _{tot} (€)	64,480	55,077	53,231	52929.97	54,366	50,582	47625.10	46318.77

Best result is in bold font.

Table 6

Main geometrical and physical results for the optimum shell-and-tube heat exchanger configuration for second case study.

	Original Design [55]	GA [11]	PSO [12]	ABC [56]	BBO [15]	OOA
D _s (m)	0.387	0.62	0.59	1.0024	0.55798	0.6306
L (m)	4.88	1.548	1.45	2.4	1.133	1.282
B (m)	0.305	0.44	0.423	0.354	0.5	0.399
d _o (m)	0.013	0.016	0.0145	0.0103	0.01	0.0175
N _t	160	803	894	704	1565	900
v _f (m/s)	1.76	0.68	0.74	0.36	0.898	0.848
R _{e_f}	36,400	9487	9424	–	7804	10,000
P _{r_f}	6.2	6.2	6.2	–	6.2	6.2
h _t (W/m ² K)	6558	6043	5618	4438	9180	8246
ΔP _t (Pa)	62,812	3673	4474	2046	4176	3533
d _e (m)	0.013	0.011	0.0103	–	0.0071	0.0085
v _s (m/s)	0.94	0.41	0.375	0.12	0.398	0.399
R _{e_s}	16,200	8039	4814	–	3515	4207
P _{r_s}	5.4	5.4	5.4	–	5.4	5.4
h _s (W/m ² K)	5735	3476	4088.3	5608	4911	4545
ΔP _s (Pa)	67,684	4365	4721	2716	5917	5486
U (W/m ² K)	1471	1121	1177	1187	1384	1326
A (m ²)	46.6	62.5	59.15	54.72	55.73	49.21
C _i (€)	16,549	19,163	18,614	17,893	18,059	16982.74
C _{od} (€)	27,440	1671	1696	1584.2	1251.5	1590.71
C _{tot} (€)	43,989	20,834	20,310	19,478	19,310	18573.45

Best result is in bold font.

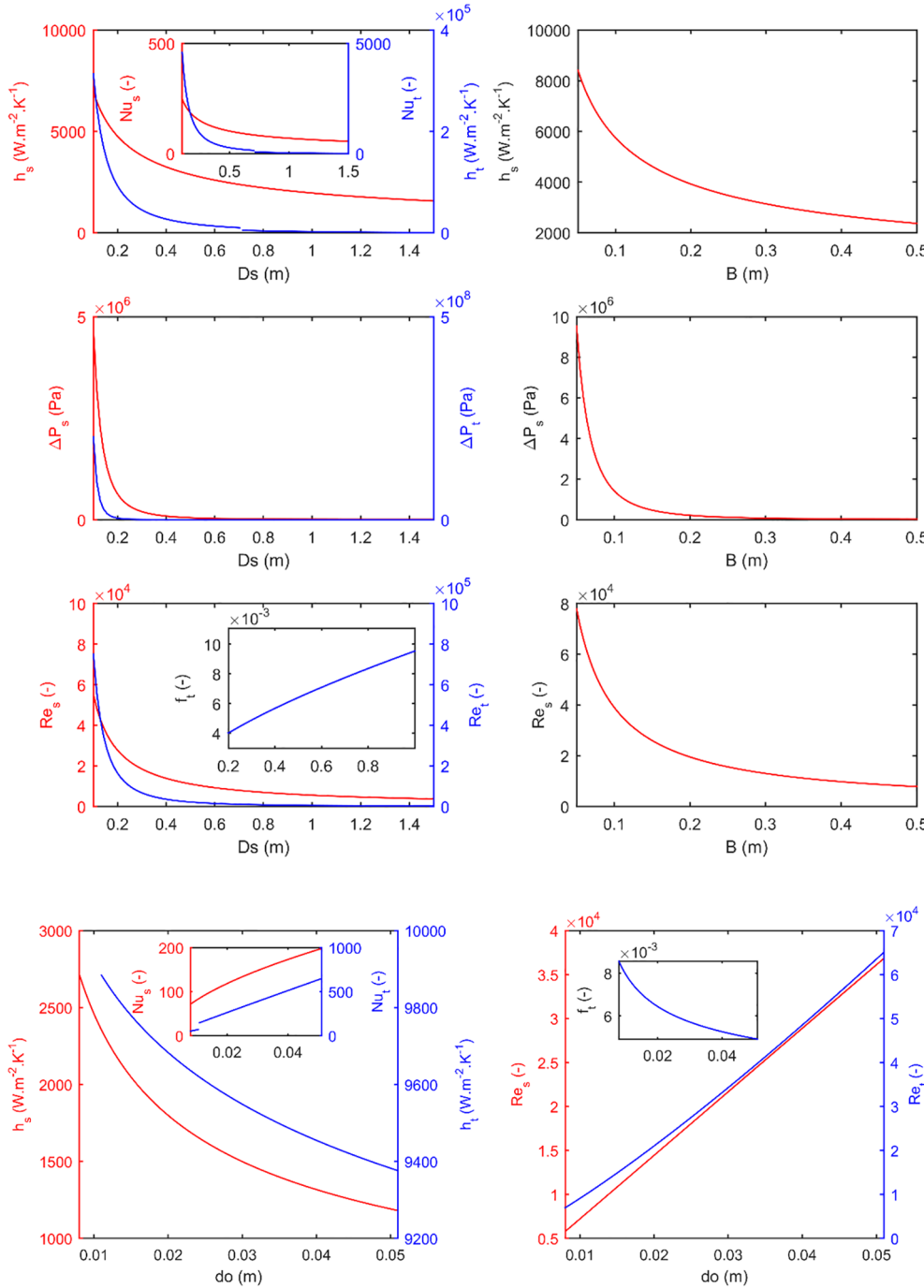


Fig. 10. Variation of the shell diameter and baffle spacing in limit range and its influence in convective heat transfer coefficients, pressure drops, Reynolds, Nusselt numbers and friction factor for the shell-and-tube heat exchanger study case 1 (red lines for shell side and blue line for tube side). (For interpretation of the references to colour in this figure legend, the reader is referred to the web version of this article.)

in comparison to the original study [41] that a reduction of 28.17% was obtained, while lower values for the variables D_s and d_o and an increase in B was achieved. Also, increases in the heat transfer coefficients for both fluids were obtained. For the comparison against a recent work [16] is made a reduction of 2.74% are obtained, while the same behavior is seen about the decision variables and heat transfer coefficients, with increase of 62% for tube fluid heat transfer coefficient and 13.92% for the shell fluid heat transfer coefficient. About pressure drops an increase for the tube side were achieved (24.3%) while a decrease of 17.98% in the shell side were obtained.

From the results it can be inferred that reductions in the heat exchanger length (L) culminate in lower value for the heat exchanger area (A), even if the number of tubes (N_t) increases and the outside diameter of the tube (d_o) decreases. The rise of the number of tubes (N_t) and the reduction of the shell diameter (D_s) result in a reduction of the flow

velocities that impact directly the pressure drops.

The results for second case study were compared to the original case design [55], Caputo et al. [11] (GA), Patel & Rao [12] (PSO), Sahin et al. [56] (ABC) and Hadidi & Nazari [15] (BBO) and are presented in Table 6. The convergence rate of the best simulation obtained with OOA reached low variation after 50 iterations (Fig. 9(b)) for this case study. In comparison to the original study [53] a reduction of 57.78% was obtained, while higher values for all the design variables. Also, increase in the heat transfer coefficient for tube side (25.74%) and reduction in the heat transfer coefficient for the shell side (20.75%) were obtained. Comparing with a more recent work [15] a reduction of 3.8% is obtained for the total cost, while reduction in B and an increasing in D_s and d_o are observed. Reductions in both heat transfer coefficients are achieved, 10.17% and 7.45% for tube and shell sides, respectively, just like the pressure drops, with reductions about 15.40% and 7.3% for

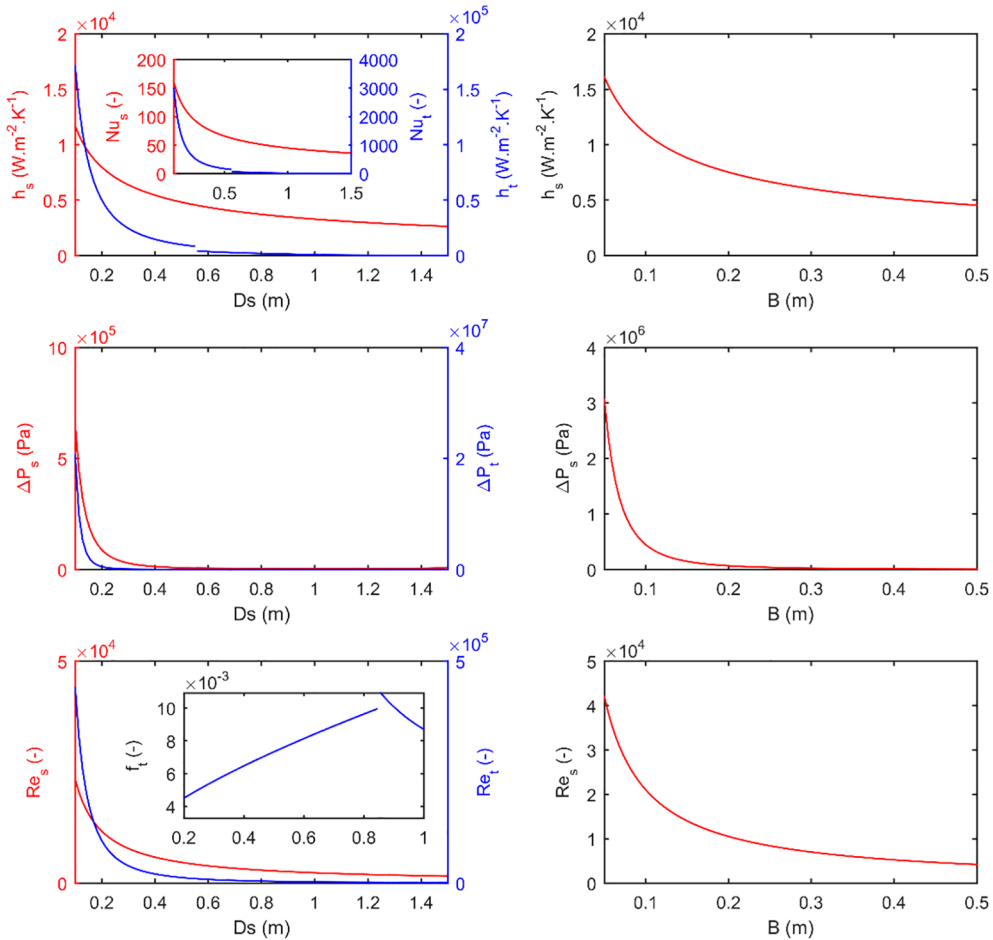
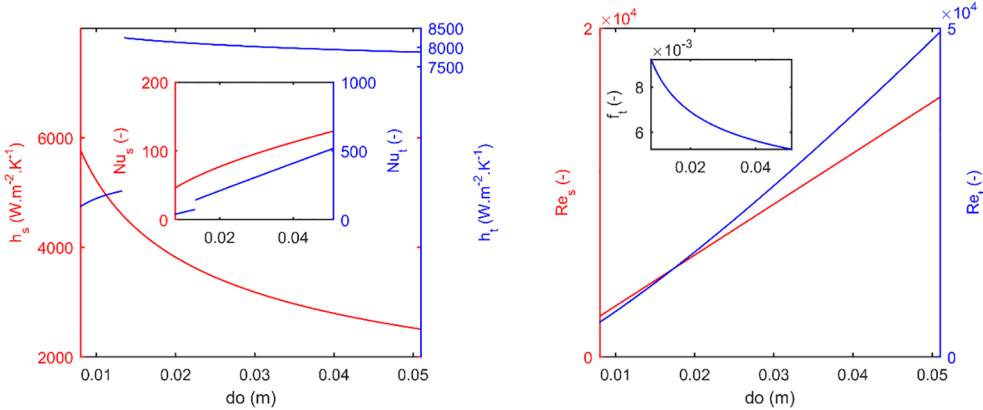


Fig. 12. Variation of the shell diameter and baffle spacing in limit range and its influence in convective heat transfer coefficients, pressure drops, Reynolds, Nusselt numbers and friction factor for the shell-and-tube heat exchanger study case 2 (red lines for shell side and blue line for tube side). (For interpretation of the references to colour in this figure legend, the reader is referred to the web version of this article.)



tube and shell sides. Also, a significant reduction in the number of tubes, about 42.49%, was reached.

In this case, an increase in the shell diameter (D_s) rise the number of tubes (N_t) result in a reduction of the investment cost (C_i) once they influence the heat exchanger length (L) and heat exchanger area (A). Also, reductions in the flow velocities impact the pressure drops, changing the operational costs (C_{od}).

A thermal-hydraulic analysis for both single-objective cases is presented in Figs. 10–13 (varying one variable design and fixing the remaining at the optimized values).

For both cases, from Figs. 10–13, it can be seen that higher values

for the shell diameter results in lower Reynolds numbers for shell due to the influence of the shell diameter in the determination of the cross-sectional area normal to flow direction and also for the tube side in the determination of the flow velocity once this parameter is dependent to the number of tubes calculation. This fact contributes to the behaviors of the convective heat transfer coefficients for shell and tube fluids, where both presents dependency with the Reynolds numbers, Nusselt numbers – dependent of the convection heat transfer coefficients – and pressure drops. Also, the decay in the Reynolds number for tube side results in an increase on the respective friction factor.

Considering the baffle spacing, this variable presented influence in

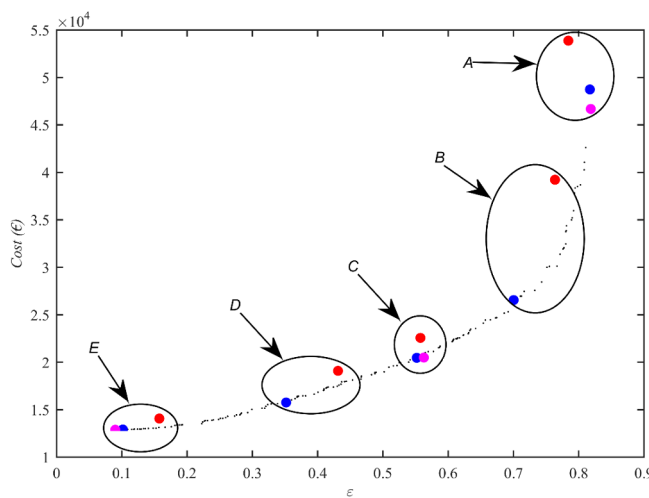


Fig. 14. Pareto front for the multi-objective shell-and-tube heat exchanger study case and sample points from A to E. Blue dots represent the evaluation points for the proposed algorithm, MOOOA, red dots represent the points for the TLBO [23] and the magenta dots represent the points for the MOFSDE [20]. (For interpretation of the references to colour in this figure legend, the reader is referred to the web version of this article.)

the shell side Reynolds number – higher values lead to lower Reynolds numbers – by the determination of the cross-sectional area normal do the flow direction, resulting in a decay behavior of the convective heat transfer coefficient and in the pressure drop. About the outside diameter of tube, a dependency with the Reynolds numbers for both shell and tube sides were observed. An increase in the outside diameter of tubes lead to higher Reynolds numbers, influencing the convective heat

transfer coefficient where a decay behavior is obtained both shell and tube sides. This behavior also impacts the Nusselt numbers of the fluids.

Regardless of the decay curve for the Reynolds numbers the flow regime tend to be maintained turbulent, leaving this situation only for values of shell diameter and baffle spacing very close to the upper boundary design variable limit. For the outside tube diameter also corroborates the previous affirmation about the flow regime once its increase only causes an increase of the Reynolds numbers values. Yet, the results for the Nusselt numbers indicates that the process in the entire range of the variables is based on convective heat transfer process.

About the multi-objective case study of a shell-and-tube heat exchanger the results for the Pareto front obtained over all the trials performed are presented in Fig. 14 and values for the decision values and objective functions for all analysis points A to E are shown in Table 7.

From Fig. 14 it can be seen that MOOOA reached points more closely linked to the Pareto Front of MOFSDE than TLBO, fact that can also be related to some convergence ability, also obtaining good distribution and spread over the objective space.

From Table 7 it can be observed that MOOOA also reached a non-dominated point with an effectiveness as high as MOFSDE for sample point A and also a total cost as low as MOFSDE for sample point E. Considering the best compromise point - sample point C – the multi-objective version of the proposed algorithm also presented values closer to the ones obtained by MOFSDE for the inside tube diameter, number of tubes, length of tubes and tube arrangement.

The results also reveal that considering the sample point C – taken as the best compromise – MOOOA reached a higher value for the shell diameter, 0.3943 m, an increase of 14.29% and 22.23% in comparison to TLBO and MOFSDE (recalculated based in the model provided), respectively. Also, decreases in both heat transfer coefficients were

Table 7
Results for the evaluation points A to E for the shell-and-tube heat exchanger.

	A	B	C	D	E	
MOOOA	ϵ Cost (€) di (m) Nt L (m) $\frac{pt}{do}$ (m) $\frac{bc}{Ds}$ (m) $\frac{bc}{Ds}$ (m) ntp t_α	0.8172 48735.95 0.0115 100 5.3224 1.6057 0.19 0.9492 1 45°	0.73 26542.03 0.0121 100 5.3712 1.6781 0.2017 0.20 1 45°	0.5517 20463.28 0.0116 255 6.8019 1.5424 0.2468 0.3755 1 45°	0.3516 15758.11 0.0112 470 6.7222 1.25 0.1954 0.2604 1 45°	0.1014 12913.55 0.0119 111 3.6516 1.4348 0.2337 0.20 1 45°
TLBO [23]	ϵ Cost (€) di (m) Nt L (m) t_α	0.7839 53887.68 0.0148 600 7.62 90°	0.7635 39219.14 0.0115 600 5.93 90°	0.5576 22564.77 0.0112 310 3.59 90°	0.4312 19097.22 0.0117 252 3 90°	0.1575 14061.76 0.0153 100 3 90°
MOFSDE [20]	ϵ Cost (€) di (m) Nt L (m) $\frac{pt}{do}$ (m) $\frac{bc}{Ds}$ (m) $\frac{bc}{Ds}$ (m) ntp t_α	0.8184 46676.6 0.01266 100 3.89569 1.79764 0.19243 0.2 3 45°	– – – – – – – – – 45°	0.5627 20487.2 0.0112 271.386 6.30851 1.25 0.19 0.2 2 45°	– – – – – – – – – 45°	0.0900 12887.6 0.0112 297.953 4.80431 1.25 0.19 0.2 1 45°

The points presented in the work of Sanaye & Hajabdollahi [19] using the NSGA-II did not present the values for the design variables, reason why these points were omitted from the comparison. However, the values for the objectives were (ϵ | Cost (€)): A (0.77119|55359), B (0.69965|33729), C (0.55044|23328), D (0.34938|17169) e E (0.15748|14109).

achieved ($3085.9 \text{ W/m}^2\text{K}$ for tube side and $247.4 \text{ W/m}^2\text{K}$ for shell side) and in the overall heat transfer coefficient ($211.59 \text{ W/m}^2\text{K}$). Also, it can be observed that MOOOA was able to reach high effectiveness value with low number of tubes, inside tube diameter and length of tubes, fact not achieved with TLBO.

The proposed algorithm showed good potential in the search for the global solution of single-objective optimizations benchmark and engineering problems, with ease implementation and low processing requirement. About the multi-objective results, the technique still needs improvement, mainly considering the need to provide better balance between the diversity in distribution and spread over the True Pareto Front from the point of view of benchmark functions, although the results obtained for the engineering problem (with good distribution and spread for the Pareto Front generated).

5. Conclusion and future research

Based on the decoy behavior of owls, a novel metaheuristic algorithm, called Owl Optimization Algorithm (OOA), is proposed in this paper. OOA is a population-based algorithm with few adjustment parameters, what turns it attractive for several applications. The results obtained showed that the proposed OOA reached better results for the benchmark functions tested for single-objective optimization, including even good processing time, in comparison to other well-known algorithms, GA and PSO. Considering the good results obtained in the single-objective optimization the proposed OOA was applied in heat exchangers shell-and-tube type for single and multi-objective optimization, achieving better results than previous works for the objective functions adopted, total cost for shell-and-tube heat exchanger in two case studies, both with 28.17% and 57.78% of enhancement in the results respectively for each case for single-objective optimization. The multi-objective case study presented that the proposed algorithm reached good distribution and spread for the non-dominated points generated over all the trials and competitive results in comparison to previous works. Future research may aim about the self-adjustment of the parameters, adopting different solutions diversity as basis, such as OBL (Opposition-Based Learning) that adopts complementary solutions, i.e. opposite solutions, allowing different exploration and exploitation of the search space or even a mechanism for the balance between the distribution and spread of the non-dominated points generated over the True Pareto Fronts in the case of benchmark functions.

Declaration of Competing Interest

The authors declare that they have no known competing financial interests or personal relationships that could have appeared to influence the work reported in this paper.

Acknowledgements

The authors would like to thank National Council of Scientific and Technologic Development of Brazil – CNPq (grant: 152503/2018-8-PDJ) for the scholarship financial support of this work, and grants: 303908/2015-7-PQ, 303906/2015-4-PQ, 404659/2016-0-Univ, 405101/2016-3-Univ) and Araucária Foundation (PRONEX – 042/2018) for financial support of this work.

References

- [1] S. Mahdavi, M.E. Shiri, S. Rahnamayan, Metaheuristics in large-scale global continuous optimization: a survey, *Inf. Sci.* 295 (2015) 407–428.
- [2] D.E. Kvasov, M.S. Mukhametshyan, Metaheuristic vs. deterministic global optimization algorithms: the univariate case, *Appl. Math. Comput.* (2017) 1–15.
- [3] X.-S. Yang, *Engineering Optimization: An Introduction with Metaheuristics Applications*, Wiley, USA, 2010.
- [4] J.H. Holland, Genetic algorithms, *Sci. Am.* 267 (1992) 66–72.
- [5] S.D. Dao, K. Abhary, R. Marian, A bibliometric analysis of genetic algorithms throughout the history, *Comput. Ind. Eng.* 110 (2017) 395–403.
- [6] Y. Zhang, S. Wang, G. Li, A Comprehensive survey on particle swarm optimization algorithm and its applications, *Math. Probl. Eng.* (2015) 38.
- [7] M. Mavrovouniotis, C. Li, S. Yang, A survey of swarm intelligence for dynamic optimization: algorithms and applications, *Swarm Evol. Comput.* 33 (2017) 1–17.
- [8] S. Salcedo-Sanz, Modern meta-heuristics based on nonlinear physics processes: a review of models and design procedures, *Phys. Rep.* 655 (2016) 1–70.
- [9] S. Ghosh, I. Ghosh, D.K. Pratihar, B. Maiti, P.K. Das, Optimum stacking pattern for multi-stream plate-fin heat exchanger through a genetic algorithm, *Int. J. Therm. Sci.* 50 (2011) 214–224.
- [10] R.K. Shah, D.P. Sekulic, *Fundamentals of Heat Exchanger Design*, John Wiley & Sons, 2003.
- [11] A.C. Caputo, P.M. Pelagagge, P. Salini, Heat exchanger design based on economic optimization, *Appl. Therm. Eng.* 28 (2008) 1151–1159.
- [12] V.K. Patel, R.V. Rao, Design optimization of shell-and-tube heat exchanger using particle swarm optimization technique, *Appl. Therm. Eng.* 30 (2010) 1417–1425.
- [13] N.M. Khalfe, S.K. Lahiri, S.K. Wadhwa, Simulated Annealing technique to design minimum cost exchanger, *Chem. Ind. Chem. Eng. Q.* 14 (4) (2011) 409–427.
- [14] A. Hadidi, M. Hadidi, A. Nazari, A new design approach for shell-and-tube heat exchangers using imperialist competitive algorithm (ICA) from economic point of view, *Energy Convers. Manage.* 67 (2013) 66–74.
- [15] A. Hadidi, A. Nazari, Design and economic optimization of shell-and-tube heat exchangers using biogeography-based (BBO) algorithm, *Appl. Therm. Eng.* 51 (2013) 1263–1272.
- [16] M. Asadi, Y. Song, B. Sundén, G. Xie, Economic optimization design of shell-and-tube heat exchangers by cuckoo-search-algorithm, *Appl. Therm. Eng.* 73 (2014) 1032–1040.
- [17] D.K. Mohanty, Application of firefly algorithm for design optimization of a shell and tube heat exchanger from economic point of view, *Int. J. Therm. Sci.* 102 (2016) 228–238.
- [18] E.H. Vasconcelos Segundo, A.L. Amoroso, V.C. Mariani, L.S. Coelho, Economic optimization design for shell-and-tube heat exchangers by a Tsallis differential evolution, *Appl. Therm. Eng.* 111 (2017) 143–151.
- [19] S. Sanaye, H. Hajabdollahi, Multi-objective optimization of shell and tube heat exchangers, *Appl. Therm. Eng.* 30 (2010) 1937–1945.
- [20] H.V.H. Ayala, P. Keller, M.F. Moraes, V.V. Matiani, L.S. Coelho, R.V. Rao, Design of heat exchangers using a novel multiobjective free search differential evolution paradigm, *Appl. Therm. Eng.* 94 (2016) 170–177.
- [21] S. Fettaka, J. Thibault, Y. Gupta, Design of shell-and-tube heat exchangers using multiobjective optimization, *Int. J. Heat Mass Transf.* 60 (2013) 343–354.
- [22] A. Ghanei, E. Assareh, M. Biglari, A. Ghanbarzadeh, Ar.R. Noghrehabadi, Thermal-economic multi-objective optimization of shell and tube heat exchanger using particle swarm optimization (PSO), *Heat Mass Transfer* 50 (2014) 1375–1384.
- [23] R.V. Rao, V. Patel, Multi-objective optimization of heat exchangers using a modified teaching-learning-based optimization algorithm, *Appl. Math. Model.* 37 (2013) 1147–1162.
- [24] G.N. Xie, B. Sundén, Q.W. Wang, Optimization of compact heat exchangers by a genetic algorithm, *Appl. Therm. Eng.* 28 (2008) 895–906.
- [25] M. Mishra, P.K. Das, S. Sarangi, Second law based optimisation of crossflow plate-fin heat exchanger design using genetic algorithms, *Appl. Therm. Eng.* 29 (2009) 2983–2989.
- [26] R.V. Rao, V.K. Patel, Thermodynamic optimization of cross-flow plate-fin heat exchanger using particle swarm optimization, *Int. J. Therm. Sci.* 49 (2010) 1712–1721.
- [27] H. Zarea, F.M. Kashkooli, A.M. Mehryan, M.R. Saffarian, E.N. Behrghani, Optimal design of plate-fin heat exchangers by a Bees Algorithm, *Appl. Therm. Eng.* 69 (2014) 267–277.
- [28] E.H. Vasconcelos Segundo, A.L. Amoroso, V.C. Mariani, L.S. Coelho, Thermodynamic optimization design for plate-fin heat exchangers by Tsallis JADE, *Int. J. Therm. Sci.* 113 (2017) 136–144.
- [29] S. Sanaye, H. Hajabdollahi, Thermal-economic multi-objective optimization of plate fin heat exchanger using genetic algorithm, *Appl. Energy* 87 (2010) 1893–1902.
- [30] H. Zarea, F.M. Kashkooli, M. Soltani, M. Rezaeian, A novel single and multi-objective optimization approach based on Bee Algorithm Hybrid with Particle Swarm Optimization (BAHPSO): application to thermal-economic design of plate fin heat exchangers, *Int. J. Therm. Sci.* 129 (2018) 552–564.
- [31] H. Najafi, B. Najafi, P. Hoseinpouri, Energy and cost optimization of a plate and fin heat exchanger using genetic algorithm, *Appl. Therm. Eng.* 31 (2011) 1839–1847.
- [32] B.D. Raja, R.L. Jhala, V. Patel, Many-objective optimization of cross-flow plate-fin heat exchanger, *Int. J. Therm. Sci.* 118 (2017) 320–339.
- [33] B.D. Raja, R.L. Jhala, V. Patel, Thermal-hydraulic optimization of plate heat exchanger: a multi-objective approach, *Int. J. Therm. Sci.* 124 (2018) 522–535.
- [34] H. Yang, J. Wen, S. Wang, Y. Li, Thermal design and optimization of plate-fin heat exchangers based global sensitivity analysis and NSGA-II, *Appl. Therm. Eng.* 136 (2018) 444–453.
- [35] M. Bidabadi, A.K. Sadaghiani, A. Vadhat Azad, Spiral heat exchanger optimization using genetic algorithm, *Scientia Iran. B* 20 (2013) 1445–2145.
- [36] O.E. Turgut, M.T. Çoban, Thermal design of spiral heat exchangers and heat pipes through global best algorithm, *Heat Mass Transfer* 53 (2017) 899–916; H.N. Coulombe, Behavior and population ecology of the burrowing owl, *Speotyto Cunicularia*, in the Imperial Valley of California, *Condor* 73 (1971) 162–176.
- [37] E.H. Vasconcelos Segundo, V.C. Mariani, L.S. Coelho, Design of spiral heat exchanger from economic and thermal point of view using a tuned wind-driven optimizer, *J. Braz. Soc. Mech. Sci. Eng.* 40 (2018) 212–224; D.H. Catlin, D.K. Rosenberg, Breeding dispersal and nesting behavior of burrowing owls following experimental nest predation, *Am. Midland Natural.* 159 (2008) 1–7.

- [38] M. Mlakar, T. Tusař, B. Filipic, Comparing solutions under uncertainty in multi-objective optimization, *Math. Probl. Eng.* 10 (2014).
- [39] K. Deb, A. Pratap, S. Agarwal, T. Meyarivan, A fast and elitist multiobjective genetic algorithm: NSGA-II, *IEEE Trans. Evol. Comput.* 6 (2) (2002) 182–197.
- [40] S. Mirjalili, A.H. Gandomi, S.Z. Mirjalili, S. Saremi, H. Faris, S.M. Mirjalili, Salp Swarm Algorithm: a bio-inspired optimizer for engineering design problems, *Adv. Eng. Softw.* 114 (2017) 163–191.
- [41] S. Mirjalili, Dragonfly algorithm: a new meta-heuristic optimization technique for solving single-objective, discrete, and multi-objective problems, *Neural Comput. Appl.* 27 (4) (2016) 1053–1073.
- [42] S.Z. Mirjalili, S. Mirjalili, S. Saremi, H. Faris, I. Aljarrah, Grasshopper optimization algorithm for multi-objective optimization problems, *Appl. Intell.* 48 (4) (2018) 805–820.
- [43] F. Martinez-Rios, A. Murillo-Suarez, A new swarm algorithm for global optimization of multimodal functions over multi-threading architecture hybridized with simulating annealing, *Proc. Comput. Sci.* 135 (2018) 449–456.
- [44] E. Zitzler, K. Deb, L. Thiele, Comparison of multiobjective evolutionary algorithms: empirical results, *Evol. Comput.* 8 (2) (2000) 173–195.
- [45] S. Huband, P. Hingston, L. Barone, L. While, A review of multiobjective test problems and a scalable test problem toolkit, *IEEE Trans. Evol. Comput.* 10 (5) (2006) 477–506.
- [46] R.K. Sinnott, J.M. Coulson, J.F. Richardson, *Chemical Engineering Design* vol. 6, Butterworth-Heinemann, Boston, USA, 1996.
- [47] S. Kakac, H. Liu, *Heat Exchangers Selection Rating, and Thermal Design*, CRC Press, New York, 2000.
- [48] M. Tall, I. Bulatov, J. Klemes, P. Stehlík, Cost estimation and energy price forecast for economic evaluation of retrofit projects, *Appl. Therm. Eng.* 23 (2003) 1819–1835.
- [49] S. Jiang, Y.S. Ong, J. Zhang, L. Feng, Consistencies and contradictions of performance metrics in multiobjective optimization, *IEEE Trans. Cybern.* 14 (2014) pps.
- [50] D.A.V. Veldhuizen, G.B. Lamont, Multiobjective evolutionary algorithms: analyzing the state-of-the-art, *Evol. Comput.* 8 (2) (2000) 125–147.
- [51] D.A. Van Veldhuizen, G.B. Lamont, Multiobjective evolutionary algorithm test suites, *Proceedings of the 1999 ACM Symposium on Applied Computing*, 1999, pp. 351–357.
- [52] E. Zitzler, L. Thiele, Multiobjective optimization using evolutionary algorithms – a comparative case study, *Proceedings of the International Conference on Parallel Solving from Nature*, 1998, pp. 292–301.
- [53] W.D. Chang, Multimodal function optimizations with multiple maximums and multiple minimums using an improved PSO algorithm, *Appl. Soft Comput.* 60 (2017) 60–72.
- [54] A. Azadeh, S. Elahi, M.H. Farahani, B. Nasirian, A genetic algorithm-Taguchi based approach to inventory routing problem of a single perishable product with transhipment, *Comput. Ind. Eng.* 104 (2017) 124–133.
- [55] D.Q. Kern, *Process Heat Transfer*, McGraw-Hill, 1950.
- [56] A.S. Sahin, B. Kilic, U. Kilic, Design and economic optimization of shell and tube heat exchangers using Artificial Bee Colony (ABC) algorithm, *Energy Convers. Manage.* 52 (2011) 3356–3362.